

Constraining the Hubble constant to a precision of about 1% using multi-band dark standard siren detections

Liang-Gui Zhu^{1,2}, Ling-Hua Xie¹, Yi-Ming Hu^{1,2*}, Shuai Liu^{1,2*}, En-Kun Li^{1,2*}, Nicola R. Napolitano¹, Bai-Tian Tang¹, Jian-Dong Zhang^{1,2}, and Jianwei Mei^{1,2}

¹School of Physics and Astronomy, Sun Yat-sen University (Zhuhai Campus), Zhuhai 519082, China;

²MOE Key Laboratory of TianQin Mission, TianQin Research Center for Gravitational Physics, Frontiers Science Center for TianQin, CNSA Research Center for Gravitational Waves, Sun Yat-sen University (Zhuhai Campus), Zhuhai 519082, China

Received October 11, 2021; accepted January 17, 2022; published online February 28, 2022

Gravitational wave signal from the inspiral of stellar-mass binary black hole can be used as standard sirens to perform cosmological inference. This inspiral covers a wide range of frequency bands, from the millihertz band to the audio-band, allowing for detections by both space-borne and ground-based gravitational wave detectors. In this work, we conduct a comprehensive study on the ability to constrain the Hubble constant using the dark standard sirens, or gravitational wave events that lack electromagnetic counterparts. To acquire the redshift information, we weight the galaxies within the localization error box with photometric information from several bands and use them as a proxy for the binary black hole redshift. We discover that TianQin is expected to constrain the Hubble constant to a precision of roughly 30% through detections of 10 gravitational wave events; in the most optimistic case, the Hubble constant can be constrained to a precision of <10%, assuming TianQin I+II. In the optimistic case, the multi-detector network of TianQin and LISA is capable of constraining the Hubble constant to within 5% precision. It is worth highlighting that the multi-band network of TianQin and Einstein Telescope is capable of constraining the Hubble constant to a precision of about 1%. We conclude that inferring the Hubble constant without bias from photo-z galaxy catalog is achievable, and we also demonstrate self-consistency using the *P-P* plot. On the other hand, high-quality spectroscopic redshift information is crucial for improving the estimation precision of Hubble constant.

gravitational wave standard siren, Hubble constant, stellar-mass binary black hole, photometric luminosity, multi-band gravitational wave detection

PACS number(s): 04.30.-w, 98.80.Es, 97.60.Lf, 98.62.Qz, 04.80.Nn

Citation: L.-G. Zhu, L.-H. Xie, Y.-M. Hu, S. Liu, E.-K. Li, N. R. Napolitano, B.-T. Tang, J.-D. Zhang, and J. Mei, Constraining the Hubble constant to a precision of about 1% using multi-band dark standard siren detections, *Sci. China-Phys. Mech. Astron.* **65**, 259811 (2022), <https://doi.org/10.1007/s11433-021-1859-9>

1 Introduction

The gravitational wave (GW) observations of compact binary coalescences can be used as standard sirens thanks to the fact

that the intrinsic GW strength can be deduced from the phase evolution [1]. When combined with redshift data from electromagnetic (EM) measurements, such standard sirens can be used to determine cosmological parameters.

The Hubble constant can be determined using data from the late Universe measurements, represented by the type Ia

*Corresponding authors (Yi-Ming Hu, email: huyiming@mail.sysu.edu.cn; Shuai Liu, email: liushuai5@mail.sysu.edu.cn; En-Kun Li, email: lienk@mail.sysu.edu.cn)

supernova (SN Ia) observations, and from the early Universe measurements, represented by the cosmic microwave background (CMB) anisotropies observations. However, there is a significant inconsistency between these two measurements, and because the inconsistency has grown over 4σ [2-9], this discrepancy, also known as the “Hubble tension”, has become a hot topic. Although luminosity distance measurements are sometimes subject to high statistical errors, they remain an important probe as the GW observation can provide a direct measurement of the luminosity distance that is independent of the cosmic distance scale ladder. Thus, standard sirens possess the potential to clarify the Hubble tension [10-13].

The direct detection of the GW signals from compact binary coalescences by Advanced LIGO and Virgo [14-27] opened an era of GW astronomy. Among different types of GW signals, the binary neutron stars (BNSs) and neutron star-black hole binaries (NSBHBs) mergers are ideal standard sirens since they have the potential to be detected through both the GW and the EM channels. The current ground-based GW detectors, including KAGRA [28] and LIGO-India [29], is expected to detect dozens of GW events of BNSs and NSBHBs during the course of the operation, and a few percent precision of the Hubble constant are expected to be reached from the GW cosmology [10, 30-32]. The first multimessenger observations of a BNS merger event GW170817 [19, 33-35] provided the first standard siren measurement of the Hubble constant, $H_0 = 69^{+17}_{-8}$ km s $^{-1}$ Mpc $^{-1}$ [36] (also see refs. [37-40]).

The stellar-mass binary black hole (SBBH) mergers should be dark in the EM channel [41, 42]; therefore, the cosmological constraint from SBBHs can only be derived through the “dark standard siren” [1, 43]. In this scenario, the redshift information is provided by matching the GW source sky localization and the galaxies catalogs. It is expected that the current ground-based GW detectors will continue to constrain the Hubble constant efficiently via SBBH GW events [10, 36, 38, 43-54], and indeed constraint of the Hubble constant has already been obtained with the observation of GW170814 and GW190814, provided a measurement precision of about 57% [36, 43-45].

Future ground-based GW detectors, such as the Einstein Telescope (ET) [55, 56] and Cosmic Explorer [57, 58], will be much more sensitive and capable of detecting GW events at higher redshift. This enables the potential of not only measuring the Hubble constant but also constraining other cosmological parameters [59-73]. Space-borne GW detectors operating in the millihertz band, such as TianQin [74] and LISA [75], can observe GW signals at cosmological distances, including massive black hole binaries (MBHBs) [76-78], extreme mass ratio inspirals [79-81], and SBBHs

[82-84]. Space-borne GW detectors are expected to have excellent capability for sky localization, which will also enable them to constrain the Hubble constant as well as other cosmological parameters [85-98].

SBBHs are very interesting GW sources due to the vast frequency range of their GW signals, which cover a wide frequency range from millihertz to kilohertz. This feature enables the SBBHs to be detectable in multiple band GW detectors [99, 100]. Space-borne GW detectors can observe the early inspiral signal while ground-based GW detectors can study the final merger. Both low and high frequency can be complimentary, with space-borne detectors capable of more precise phase information [82, 83] and ground-based detectors can accumulate higher signal-to-noise ratios (SNRs) [60], thus improving the overall parameter estimation precision of the GW source [101-104], in order to facilitate the extraction of physical/astronomical information [101, 105-109] and measurement of the expansion of the Universe [110].

We study the potential of constraining the Hubble constant with TianQin using the SBBH GW sources. Furthermore, the anticipated operation time of the various detectors allows simultaneous observation through a multi-detector network of TianQin [111, 112] and LISA [75], as well as a multi-band network of TianQin and ET [113]. Thus, we study how such networks might be used to better constrain the Hubble constant.

This paper is organized as follows. In sect. 2, we present the cosmological analytical framework and the methods needed to spatially localize GW sources and weight candidate host galaxies. In sect. 3, we introduce the necessary astrophysical context for the simulations and present the method for simulating observational data. In sect. 4, we illustrate the constraint processes of the cosmological parameters and show the constraint results on the Hubble constant. In sect. 5, we discuss several critical concerns raised by the analyses and simulations. In sect. 6, we summarize our results and discuss the need for additional research.

2 Methodology

Throughout the work, we adopt a spatially-flat Lambda cold dark matter (Λ CDM) cosmology. The Hubble parameter, which describes the expansion rate of the scale factor in the late Universe, can be expressed as:

$$H(z) = H_0 \sqrt{\Omega_M(1+z)^3 + \Omega_\Lambda}, \quad (1)$$

where $H_0 \equiv H(z=0)$ is the Hubble constant that describing the current rate of expansion, and $\Omega_M, \Omega_\Lambda = 1 - \Omega_M$ are the fractional densities of total matter and dark energy with respect to the critical density $\rho_c = 3H_0^2/(8\pi G)$ (where G is

Newton's gravitational constant). According to this cosmology predicts that the luminosity distance D_L of a source with redshift z is

$$D_L = c(1+z) \int_0^z \frac{1}{H(z')} dz', \quad (2)$$

where c is the speed of light in a vacuum. Throughout this work, we utilize the injected true numbers $H_0 = 67.8 \text{ km s}^{-1} \text{ Mpc}^{-1}$ and $\Omega_M = 0.307$ [2].

2.1 Standard siren and dark standard siren

The two polarizations of GW signal of an inspiralling binary with component masses m_1 and m_2 can be described as [114]:

$$h_+(t) = \left(\frac{GM_z}{c^2}\right)^{5/3} \left(\frac{\pi f(t)}{c}\right)^{2/3} \frac{2(1+\cos^2\iota)}{D_L} \cos(\Psi(t, M_z, \eta)), \quad (3a)$$

$$h_\times(t) = \left(\frac{GM_z}{c^2}\right)^{5/3} \left(\frac{\pi f(t)}{c}\right)^{2/3} \frac{4\cos\iota}{D_L} \sin(\Psi(t, M_z, \eta)), \quad (3b)$$

where $M_z = (1+z)\mathcal{M} = (1+z)(m_1 m_2)^{3/5}/(m_1 + m_2)^{1/5}$ is the redshifted chirp mass (with a perfect degeneracy between the redshift and the physical mass), $\eta = m_1 m_2 / (m_1 + m_2)^2$ is the symmetric mass ratio, ι is the inclination angle of the binary orbital angular momentum relative in the line of sight, and $\Psi(t, M_z, \eta)$ is the phase of the GW signal. Notably, the overall amplitude is determined solely by the redshifted chirp mass, the inclination, and the luminosity distance. By observing the GW phase evolution, the mass parameter M_z can be reliably estimated, and the inclination angle can be determined by observing the amplitude ratio of different polarizations. Therefore, compact binary coalescences are referred to as "standard sirens", as it is possible to infer the luminosity distance D_L directly from the GW data.

To determine the cosmological parameters, one must still have redshift information, which the GW data analysis can only supply infrequently. The next section discusses several methods for obtaining redshift information [115]:

- The EM counterpart. The coalescence of BNS and neutron star-black hole binaries (NSBHBs) are frequently accompanied by EM radiation such as short Gamma ray bursts [35, 116, 117] or kilonovae [118-120], the redshift can be measured directly [31, 37, 39].
- The "dark standard siren". Galaxies are clustered on a small scale. Assuming the GW sources are linked with a host galaxy, one can obtain a statistical understanding of the redshift from galaxy information even in the absence of an EM counterpart [43, 44, 46, 48, 50, 87, 95, 96, 98].
- The neutron star mass distribution. EM observations, which deduced a relatively narrow distribution for neutron

star masses in BNSs. This intrinsic distribution can be exploited to overcome the mass-redshift degeneracy [47, 61, 65, 121].

- The tidal deformation of the neutron stars. During coalescence, a compact object with finite size will experience tidal deformation, resulting in phase correction of the GW waveform. Because the degree of tidal deformation is determined by both the intrinsic mass and the equation of the state of the neutron star, the correcting phase can overcome the mass-redshift degeneracy [63, 64].

- The cross-correlation method. After EM observations have mapped the spatial distribution of the galaxies in redshift space, and GW detections can also map out the spatial distribution of the GW events in luminosity distance space, then the cross-correlation of spatial distributions between the galaxies and the GW sources can be used to extract redshift information [51, 122-125].

- Other methods. There are also efforts to use the mass distribution of the SBBH population [49, 72], the intrinsic redshift probability distribution of compact binary mergers [126, 127], and high-order correction of the GW waveform phase caused by cosmic acceleration [128-130], to break the degeneracy and obtain the redshift information.

In this work, we consider the dark standard siren scenario with SBBHs to constrain the Hubble constant H_0 .

2.2 Bayesian framework

We adopt a Bayesian analytical framework to estimate cosmological parameters using the data from the dark standard siren and the catalogs of survey galaxies [10, 37, 38, 92]. Consider a set of GW detection data composed of N GW events $\mathcal{D}_{\text{GW}} \equiv \{d_{\text{GW}}^1, d_{\text{GW}}^2, \dots, d_{\text{GW}}^i, \dots, d_{\text{GW}}^N\}$ as well as the corresponding EM observation data set $\mathcal{D}_{\text{EM}} \equiv \{d_{\text{EM}}^1, d_{\text{EM}}^2, \dots, d_{\text{EM}}^i, \dots, d_{\text{EM}}^N\}$, the posterior probability distribution of the cosmological parameter set $\mathbf{H} \equiv \{H_0, \Omega_M\}$ is given by

$$\begin{aligned} p(\mathbf{H}|\mathcal{D}_{\text{GW}}, \mathcal{D}_{\text{EM}}, I) &= \frac{p_0(\mathbf{H}|I)p(\mathcal{D}_{\text{GW}}, \mathcal{D}_{\text{EM}}|\mathbf{H}, I)}{p(\mathcal{D}_{\text{GW}}, \mathcal{D}_{\text{EM}}|I)} \\ &= \frac{p_0(\mathbf{H}|I) \prod_i p(d_{\text{GW}}^i, d_{\text{EM}}^i|\mathbf{H}, I)}{p(\mathcal{D}_{\text{GW}}, \mathcal{D}_{\text{EM}}|I)}, \end{aligned} \quad (4)$$

where $p_0(\mathbf{H}|I)$ is the prior probability distribution for \mathbf{H} , I indicates all the relevant background information. The normalization factor $p(\mathcal{D}_{\text{GW}}, \mathcal{D}_{\text{EM}}|I)$ from which is independent of \mathbf{H} is also known as Bayes evidence. Therefore, we can derive from

$$p(\mathbf{H}|\mathcal{D}_{\text{GW}}, \mathcal{D}_{\text{EM}}, I) \propto p_0(\mathbf{H}|I) \prod_i p(d_{\text{GW}}^i, d_{\text{EM}}^i|\mathbf{H}, I). \quad (5)$$

For a GW event, with the corresponding GW data d_{GW}^i and the EM data d_{EM}^i , the likelihood can be expressed as:

$$p(d_{\text{GW}}^i, d_{\text{EM}}^i | \mathbf{H}, I) = \frac{\int p(d_{\text{GW}}^i, d_{\text{EM}}^i, D_L, z, \alpha, \delta | \mathbf{H}, I) dD_L dz d\alpha d\delta}{\beta(\mathbf{H}|I)}, \quad (6)$$

where α and δ represent the longitude and latitude, respectively. To eliminate systematic biases due to the selection effect, we introduced a correction term $\beta(\mathbf{H}|I)$ as the denominator [10, 37, 131]. The integrand in the numerator of eq. (6) can be factorized as:

$$\begin{aligned} & p(d_{\text{GW}}^i, d_{\text{EM}}^i, D_L, z, \alpha, \delta | \mathbf{H}, I) \\ &= p(d_{\text{GW}}^i | D_L, z, \alpha, \delta, \mathbf{H}, I) p_0(D_L, z, \alpha, \delta | \mathbf{H}, I) \\ &= p(d_{\text{GW}}^i | D_L, \alpha, \delta, I) p(d_{\text{EM}}^i | z, \alpha, \delta, I) p_0(D_L, z, \alpha, \delta | \mathbf{H}, I) \\ &= p(d_{\text{GW}}^i | D_L, \alpha, \delta, I) p(d_{\text{EM}}^i | z, \alpha, \delta, I) \\ &\quad \times p_0(D_L | z, \mathbf{H}, I) p_0(z, \alpha, \delta | \mathbf{H}, I), \end{aligned} \quad (7)$$

where p_0 represents the prior.

Assuming that the GW noise is Gaussian and stationary, one has [132]

$$\begin{aligned} & p(d_{\text{GW}}^i | D_L, \alpha, \delta, I) \\ &= \int p(d_{\text{GW}}^i | D_L, \alpha, \delta, \theta', I) d\theta' \\ &\propto \int \exp\left(-\frac{1}{2}\langle d_{\text{GW}}^i - h(D_L, \alpha, \delta, \theta') | d_{\text{GW}}^i - h(D_L, \alpha, \delta, \theta') \rangle\right) \\ &\quad \times d\theta', \end{aligned} \quad (8)$$

where $\langle \cdot | \cdot \rangle$ is the inner product as defined in eq. (18), h is the waveform of the GW signal, and θ' represents the parameters of the GW source that is unrelated to the cosmological inference. It should be noted that we marginalize over the parameters of the GW source parameters that are not directly related to the constraining cosmological parameters, such as the inclination angle ι . For the dark standard siren scenario, since we assume no EM signal associated with the GW event, we set $p(d_{\text{EM}}^i | z, \alpha, \delta, I) = \text{const.}$ [10, 38]. We assume that $p_0(D_L | z, \mathbf{H}, I) \equiv \delta(D_L - \hat{D}_L(z, \mathbf{H}))$ under the cosmology, where $\hat{D}_L(z, \mathbf{H})$ is defined in eq. (2).

In the EM observations, the sky localization of the galaxy is very accurate (relative to the sky localization of GW source), and for a galaxies catalog from a photometric sky survey, the prior $p_0(z, \alpha, \delta | \mathbf{H}, I)$ in eq. (7) can be expressed as:

$$p_0(z, \alpha, \delta | \mathbf{H}, I) = \sum_{j=1}^{N_{\text{gal}}} W_j P(z | \bar{z}_j, \sigma_{z;j}) \delta(\alpha - \alpha_j) \delta(\delta - \delta_j), \quad (9)$$

where N_{gal} is the total number of the galaxies catalog, and $P(x | \bar{x}, \sigma_x)$ is a Gaussian distribution on x , with expectation

\bar{x} and standard deviation σ_x , $x = \{z, L\}$, and W_j is the weight of galaxy, reflect a priori confidence that the galaxy could host a compact binary. While the metallicity, morphology, and rate of star formation could be different by a lot, one can assume that the potential for each galaxy to host a compact binary is the same, i.e., $W_j = 1/N_{\text{gal}}$. Alternatively, one may expect the compact binary merger rate to be proportional to the galaxy stellar mass M , which is in turn related to its luminosities in various bands, i.e., $W_j \propto M_j \simeq \hat{M}(P(L | \bar{L}_j^1, \sigma_{L;j}^1), P(L | \bar{L}_j^2, \sigma_{L;j}^2), \dots, P(L | \bar{L}_j^k, \sigma_{L;j}^k), \dots, P(L | \bar{L}_j^{N_{\text{band}}}, \sigma_{L;j}^{N_{\text{band}}}))$, where \bar{L}_j^k and $\sigma_{L;j}^k$ are the mean value and standard deviation, respectively, of the luminosity of j -th galaxy in k -th band. The variable N_{band} represents the total number of bands in the photometric sky surveys, and more details about the function $\hat{M}(\dots, P(L | \bar{L}_j^k, \sigma_{L;j}^k), \dots)$ is described in sect. 2.4.

Taking the preceding analysis into account, substituting eq. (7) into eq. (6) and marginalizing over the parameter D_L , eq. (6) becomes

$$p(d_{\text{GW}}^i, d_{\text{EM}}^i | \mathbf{H}, I) = \frac{\int p(d_{\text{GW}}^i | \hat{D}_L(z, \mathbf{H}), \alpha, \delta, I) p_0(z, \alpha, \delta | \mathbf{H}, I) dz d\alpha d\delta}{\beta(\mathbf{H}|I)}. \quad (10)$$

Following the statistical method presented in ref. [92] for evaluating the survey galaxies catalog's selection biases, we use a smooth prior distribution of the catalog redshift as:

$$p_c(z | \mathbf{H}, I) \propto \frac{1}{2\Delta z} \int_{(z-\Delta z)}^{(z+\Delta z)} \iint_{4\pi} p_0(z', \alpha, \delta | \mathbf{H}, I) d\alpha d\delta dz', \quad (11)$$

where Δz is chosen to be much larger than the redshift interval of the galaxy clusters. The correction term $\beta(\mathbf{H}|I)$ in eq. (10) can be written approximately as:

$$\beta(\mathbf{H}|I) \approx \int p(d_{\text{GW}}^i | \hat{D}_L(z, \mathbf{H}, I) p_c(z | \mathbf{H}, I) dz. \quad (12)$$

Notice that for catalogs that are composed of from multiple sources, like the GLADE catalog [133], in order to maintain self-consistency, one needs to take extra care to deal with the selection effects $p_c(z | \mathbf{H}, I)$ separately for different sources.

2.3 Localization and distance of GW source

For regular triangular space-borne GW detectors like Tian-Qin and LISA, the recorded signal can be expressed as [76, 83]:

$$h(t) = \frac{\sqrt{3}}{2} (F^+(t)h_+(t + t_D) + F^\times(t)h_\times(t + t_D)), \quad (13)$$

$$t_D \approx -\frac{R_0}{c} \sin \theta'_S \cos (\phi_d(t) - \phi'_S), \quad (14)$$

where t is the heliocentric coordinate system (HCS) time, t_D is the time delay between the solar system barycenter to the detector, $R_0 = 1$ AU, the primed angles θ'_S and ϕ'_S are the altitude and azimuth of the GW source in the HCS respectively, quantities related to the source are labeled with subscript “S”, the ones related to the detector are labeled with subscript “d”. We have $\phi_d(t) = 2\pi t/T + \phi_0$, where $T = 1$ yr is the orbital period of the detector around the Sun, ϕ_0 is the initial orbital phase of the detector at $t = 0$. In the relatively low frequency region, $f \ll f_* = c/(2\pi L)$ (where L is the arm length of the interferometer), the antenna pattern functions $F^{+,\times}(t)$ can be approximately expressed as [134]:

$$\begin{aligned} F^+(t) &= \frac{1}{2} (1 + \cos^2 \theta_S(t)) \cos 2\phi_S(t) \cos 2\psi_S(t) \\ &\quad - \cos \theta_S(t) \sin 2\phi_S(t) \sin 2\psi_S(t), \end{aligned} \quad (15a)$$

$$\begin{aligned} F^\times(t) &= \frac{1}{2} (1 + \cos^2 \theta_S(t)) \cos 2\phi_S(t) \sin 2\psi_S(t) \\ &\quad + \cos \theta_S(t) \sin 2\phi_S(t) \cos 2\psi_S(t), \end{aligned} \quad (15b)$$

where $\theta_S(t)$, $\phi_S(t)$, and $\psi_S(t)$ are the altitude, azimuth, and polarization angles, respectively, in the detector-based coordinate system at t . In comparison with eqs. (15a) and (15b), the azimuth angle of the antenna pattern functions the second independent channel differ by $+\pi/4$ for TianQin and LISA; and by $+2\pi/3$ and $+4\pi/3$ for the second and third independent laser interferometer, respectively, for ET reference [135]. This difference is due to the fact that ET unlike space-borne detectors, uses an independent interferometer. The variation of $\theta_S(t)$, $\phi_S(t)$, and $\psi_S(t)$ with time dependent on the motion of the detector in space, the detailed description of the detector’s response to the GW signals can be found in refs. [83, 136] for TianQin, in refs. [137, 138] for LISA, and in refs. [56, 139] for ET.

Notice that although in the relatively high frequency range of $f \gtrsim f_*$, the low frequency limit is no longer valid for TianQin and LISA, and the sensitivity would drop in higher frequencies. It will cause some complexity for data analysis. However, as long as we absorb the effect into the sensitivity curve, the majority of the conclusions discussed in our study remain intact [78, 83, 140]. Moreover, a full analytical formula for the frequency response of a space-based detector is given in ref. [141].

With N independent detectors observing the same GW source, the GW signals detected by different detectors can be collectively expressed as a vector,

$$\mathbf{h} = [h_1, h_2, \dots, h_k, \dots, h_N]^T, \quad (16)$$

where h_k represents the GW strain recorded by the k -th detector. The total SNR ρ of a GW source provided by multiple independent detectors is defined as:

$$\rho = \sqrt{\langle \mathbf{h} | \mathbf{h} \rangle}, \quad (17)$$

where the inner product is defined as [132, 142]:

$$\langle \mathbf{h} | \mathbf{h} \rangle = \sum_k \langle h_k | h_k \rangle \equiv \sum_k 4\Re e \int_0^\infty \frac{\tilde{h}_k^*(f) \tilde{h}_k(f)}{S_{n,k}(f)} df, \quad (18)$$

where $\tilde{h}_k(f)$ is the Fourier transform of $h_k(t)$, $*$ represents complex conjugate, and $S_{n,k}(f)$ is the sensitivity curve functions of the k -th detector. The sensitivity curves of TianQin [78, 83], LISA [140], and ET (ET-D) [56, 113, 143] are shown in Figure 1.

For a GW source characterized by a parameter set of $\boldsymbol{\theta} \equiv (\mathcal{M}_z, \eta, D_L, \alpha, \delta, \iota, t_c, \Psi_c, \psi)$ detected from multiple independent detectors, the Fisher information matrix (FIM) can provide a Cramér-Rao lower bound on the parameter estimation uncertainty [144]. The FIM is defined as follows:

$$\Gamma_{mn} \equiv \left\langle \frac{\partial \mathbf{h}}{\partial \theta_m} \middle| \frac{\partial \mathbf{h}}{\partial \theta_n} \right\rangle = \sum_k \left\langle \frac{\partial h_k}{\partial \theta_m} \middle| \frac{\partial h_k}{\partial \theta_n} \right\rangle, \quad (19)$$

where θ_m indicates the m -th parameter of the GW event. The covariance matrix Σ equals to the inverse of the FIM, $\Sigma = \Gamma^{-1}$, we can adopt $\Delta\theta_m = \sqrt{\Sigma_{mm}} = \sqrt{(\Gamma^{-1})_{mm}}$ as the estimation error of the parameter, with the sky localization error being $\Delta\Omega = 2\pi |\sin \delta| \sqrt{\Sigma_{\alpha\alpha} \Sigma_{\delta\delta} - \Sigma_{\alpha\delta}^2}$.

2.4 Galaxy weighting

Assuming that the formation rate of the SBBH per unit stellar mass is uniform across all galaxies, we can expect that the probability of a galaxy hosting the SBBH is proportional to its total stellar mass.

The K -band luminosity is a commonly used parameter to account for the galaxy’s mass. The K -band is commonly accepted to trace the galaxy’s old stellar population and, thus,

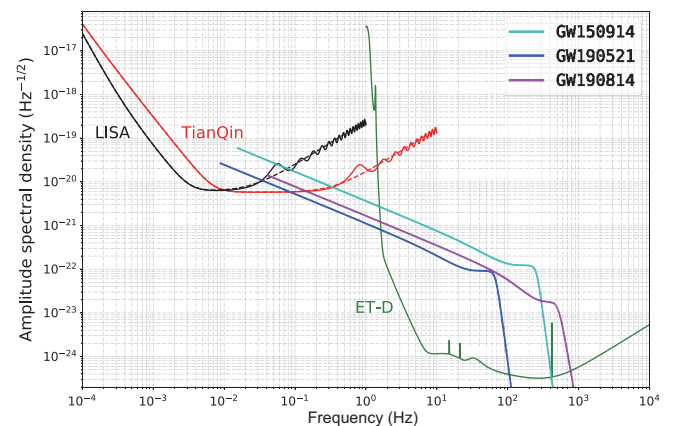


Figure 1 (Color online) Anticipated sensitivity curves for TianQin (red line), LISA (black line), and ET-D (green line). Additionally, the amplitude spectra densities $\sqrt{f}|\tilde{h}(f)|$ of GW150914 [14] (cyan line), GW190521 [23] (blue line), and GW190814 [24] (magenta line) detected by Advanced LIGO and Virgo, assuming a 5 years merger time.

is approximately proportional to the galaxy's stellar mass, as well as being weakly correlated with the galaxy's color [145, 146]. Following this logic, the K -band luminosity weighting method was applied to the dark standard siren cosmological analysis using LIGO&Virgo data [36, 38, 50]¹⁾.

In this work, we aim to adopt a different approach to improve the galaxy weighting process in order to obtain more accurate cosmological parameter estimation. This is achieved by deriving the galaxy's stellar masses from the multi-band photometry of the galaxy samples.

2.4.1 Galaxy sample and the completeness of the catalog

We use the Gravitational Wave Events in Sloan (GWENS) galaxy catalog²⁾ [36], which has been assembled on purpose for the EM-GW multimessenger observations. It uses the Sloan Digital Sky Survey (SDSS) Data Release 14 (DR14) [147], which maps over 45 million galaxies, covering about a quarter of the whole sky. The GWENS catalog provides photometric information in five bands of $ugriz$ for all galaxies, corresponding to $cModel$ magnitudes (see SDSS DR14 paper [147]) corrected for Galactic extinction from [148]. Additionally, the GWENS catalog contains photometric redshifts (photo- z) for the majority of the sample (about 98.5%) and spectroscopic redshifts for a small portion.

The completeness of a galaxy catalog plays a vital role in the dark standard of siren study. Figure 2 shows the relative completeness fraction of the GWENS catalog at different redshifts. This is obtained by using the galaxy luminosity distribution within $z < 0.05$ as the fiducial distribution, assuming that galaxies are distributed uniformly in the co-moving volume, and neglecting the evolution of the galaxy luminosity distribution with redshift. According to previous GW forecast studies [83] conclude that the SBBH inspirals detectable by TianQin are mainly concentrated in the $z < 0.2$, region with the highest redshift not exceeding $z = 0.3$. The GWENS catalog has a relative completeness fraction of around 0.63 at $z = 0.2$ and 0.37 at $z = 0.3$ in terms of the number of galaxies; however, in terms of the total luminosity contributed by galaxies, the relative completeness fraction remains above 0.9 at $z = 0.2$ and equal to or greater than 0.8 at $z = 0.3$. These levels of relative completeness ensure that the majority of host galaxies for GW sources are included in the list, and the GWENS catalog meets our requirements. There exist other galaxy catalogs available, such as the GLADE catalog [133] and the DES catalog [149–151]; however, we chose the GWENS catalog due to its higher completeness and broader sky coverage.

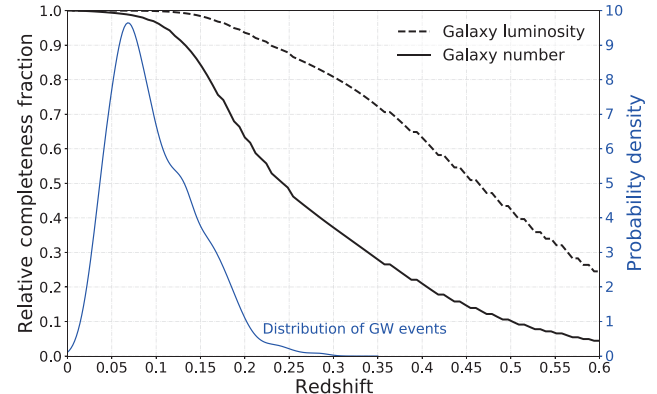


Figure 2 (Color online) The solid and dashed black lines represent completeness fractions of the GWENS catalog relative to local values, in terms of number and luminosity (in z -band), respectively. The blue line represents the probability distribution of simulated detectable GW events, with the scales shown on the right side.

2.4.2 Stellar masses

Galaxy masses are calculated using Le Phare, a widely used spectral energy distribution (SED) fitting software [152, 153]. Le Phare matches observed galaxy colors to predicted colors using a set of theoretical SED libraries derived from simple stellar population models, characterized by a series of stellar parameters such as age τ , metallicity Z , and a star formation history. The SED is convolved with the filter transmission curves (including instrument efficiency) adopted for the specific observation dataset in order to provide synthetic luminosities in the chosen bands. The best-fit parameters are obtained via minimizing the χ^2 difference between the synthetic color SED and the photometric data. The input data set is made up of multi-band photometric magnitudes from the GWENS catalog [36]. The output data set consists of the best stellar population parameters, such as age, metallicity, rate of star formation, and stellar mass. We adopt stellar templates from ref. [154] in the simple stellar population models, together with an initial mass function from ref. [155] and an exponentially decaying star formation history. We use a diverse collection of models with three metallicities ($0.005Z_{\odot}$, Z_{\odot} , and $2.5Z_{\odot}$) and different ages ($\tau \leq \tau_{\max}$), with the maximum age τ_{\max} , set by the age of the Universe at the redshift of the galaxy, with a maximum value at $z = 0$ of 13.5 Gyr. We also consider internal extinction using the models from ref. [156]. Finally, in the Le Phare run, we fix the galaxy redshift to the median of the probability density function of photo- z reported in the GWENS catalog to reduce degeneracies between redshift and galaxy colors. Figure 3 shows the final distribution of stellar masses for the

1) The B -band luminosity information is also used, which reflects the star formation rate of the galaxy.

2) The GWENS catalog is available at https://astro.ru.nl/catalogs/sdss_gwgalcat.

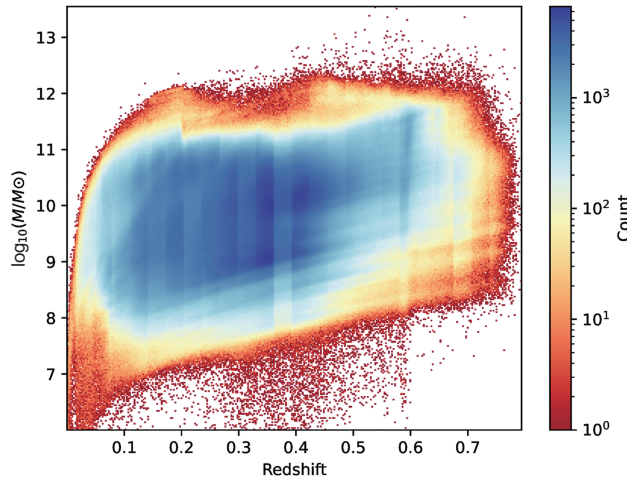


Figure 3 (Color online) Distribution of total stellar masses for GWENS galaxies derived from the Le Phare software. Note that the redshift in horizontal coordinates represents the median of the posterior probability distribution of the photo- z of galaxies.

45 141 307 GWENS galaxies. The stellar masses range, from dwarf-like systems ($\sim 10^7 M_\odot$) to massive galaxies ($\sim 10^{12} M_\odot$), as do the redshifts (from $z = 0$ to $z \sim 0.8$).

To check the presence of biases in our mass estimates, we compare them to those obtained for SDSS DR 12 (Portsmouth SED-fit Stellar Masses, which is a catalog of stellar masses of 1489670 systems from the Portsmouth Group³⁾, see also ref. [157]), for which we have discovered an overlap of ~ 53700 galaxies with GWENS. The mean deviation between our estimates and the SDSS “starburst model” catalog is $\Delta_M = 0.14$ and the scatter $\sigma_M = 0.32$ in logarithmic space, meaning that the two stellar mass estimates are basically consistent with each other (note that in the case we compared against the Portsmouth passive model catalog, we obtained a $\Delta_M = -0.07$ and scatter $\sigma_M = 0.18$). The scatter obtained by these comparisons is quite small considering the two approaches’ rather different models (e.g., refs. [158, 159] templates, no reddening, and a different magnitude definition).

3 Simulations

To perform a quantitative analysis of the Hubble constant constraint imposed by GW signals using future space-borne and ground-based GW detectors, we first simulate a GW event catalog, then identify candidate host galaxies according to the spatial localization of the GW source, and finally obtain their statistical redshift information.

3.1 Stellar-mass black hole binary signals

We adopt the “Power Law + Peak” model to populate the SBBH simulation [160]. Based on the 50 GW events published by the first (GWTC-1) [20] and the second Gravitational-Wave Transient Catalog (GWTC-2) [25], this mode has been associated with the highest Bayesian factor [160]. The model includes a power-law mass distribution for the primary component, with a smooth truncation at the lower mass limit and a Gaussian peak at the high mass end to account for the pile-up effect of pulsational pair-instability supernovae [160, 161]. The mass ratio q , which describes the ratio between the secondary component mass and the primary component mass, is modeled by a power law [162–164], $p(q|m_1) \propto q^{\beta_q}$, and $\beta_q = 1.3_{-1.6}^{+2.4}$ [160]. According to ref. [160], we adopt the associated SBBH merger rate as $R_{\text{SBBH}} = 58_{-29}^{+54} \text{ Gpc}^{-3} \text{ yr}^{-1}$ ⁴⁾, which assumes that $m_1 \geq 2M_\odot$ and includes GW190814.

Moreover, we ignore the spins of inspiralling SBBHs because the black hole spin effect has a negligible effect on the GW cosmology study [165, 166]. The eccentricity of the SBBH, which is not well constrained by LIGO and Virgo observations, should have non-negligible effects on space-borne GW detections. Throughout this work, we set the eccentricity to $e_0 = 0.01$ at GW frequency equal to 0.01 Hz as a representative value [83, 166].

Furthermore, we assume that SBBHs are uniformly distributed in the co-moving volume. Each GW event is hosted randomly in a galaxy from the GWENS catalog, assuming that the probability of each galaxy being hosted by a GW event is proportional to its total stellar mass. The orientation parameter distribution is chosen to be isotropic, i.e., $\alpha \in U[0, 2\pi]$, $\cos \delta \in U[-1, 1]$, $\alpha_L \in U[0, 2\pi]$, and $\cos \delta_L \in U[-1, 1]$; the spins are fixed at $\chi_{1,2} \equiv 0$; the remaining parameters are assumed to obey uniform distribution, $t_c \in U[0, 20]$ yr, and $\Phi_c \in U[0, 2\pi]$. Finally, we produce the simulated GW signals with the IMRPhenomPv2 waveform [167].

3.2 Detections with GW detectors

In this work, we investigate different detector configurations, including those using space-borne and ground-based GW detectors, as described below,

- TianQin: the default situation in which three satellites form a constellation and operate in a “3 months on+3 months off” mode, with a mission life time of 5 years [74];
- TianQin I+II: twin constellations of satellites with per-

3) Available at https://www.sdss.org/dr12/spectro/galaxy_portsmouth/.

4) Notice that a revised version reports an updated value of $R_{\text{SBBH}} = 52_{-26}^{+52} \text{ Gpc}^{-3} \text{ yr}^{-1}$.

pendicular orbital planes, that operates in a relay mode and can avoid the 3 months gap in data [78, 83, 168];

- TianQin+LISA: a multi-detector GW detector network of TianQin and LISA, we adopt LISA configuration according to refs. [75, 140], and considering 4 years of overlap in operation time;
- TianQin I+II+LISA: similar to above but with the TianQin I+II configuration considered;
- TianQin+ET: a multi-band GW detector network of TianQin and ET, with 5 years of overlap in operation time, we adopt ET configuration according to refs. [55, 113, 143], and assume they will continue operating for 15 years after the end of the TianQin mission;
- TianQin I+II+ET: similar to TianQin+ET but with the TianQin I+II configuration considered.

In Table 1, we list the anticipated detection rates with respect to different detection thresholds for SBBH inspirals that merge within 20 years from the start of TianQin detection. Throughout this work, we adopt two SNR thresholds for different detector configurations, one with $\rho_{\text{thre}} = 8$ for space-borne GW detectors [82, 83], including TianQin, TianQin I+II, TianQin+LISA, and TianQin I+II+LISA; and the other with $\rho_{\text{thre}} = 5$ for multi-band GW detections [103, 106], such as TianQin+ET and TianQin I+II+ET. It is worth mentioning that, for sources with $\rho \geq 5$ detected with space-borne GW detectors/networks, they can all be detected by ET with $\rho \gtrsim 20$, as long as ET is operating when they merge. Therefore we do not list the detection rate of ET separately in Table 1, and we do not consider GW sources that can only be detected by ET in this work.

The precision of the Hubble constant constrained by GW signals from SBBHs mainly depends on the spatial localization errors of the GW sources. In Figure 4, we illustrate the marginalized distribution on relative error of luminosity distance σ_{D_L}/D_L and sky localization $\Delta\Omega$. Due to the fact that GW events are useful for reconstructing the “ D_L -z relation” only when the luminosity distance can be reasonably estimated, we only include the GW sources with $\sigma_{D_L}/D_L < 0.6$ (approximately corresponding to $\Delta D_L/D_L < 1$ at the confi-

dence level of 90%) for consideration in this work.

We observe that for events detected by TianQin or TianQin I+II, the relative error of the luminosity distance for most GW sources is greater than 0.1, but the sky position of most GW sources can be localized to better than 1 deg^2 . The network of TianQin (or TianQin I+II) and LISA can marginally improve the spatial localization of the GW sources. This is because TianQin has better sensitivity than LISA at higher frequencies, which is where the SBBH inspiral signals are concentrated.

On the other hand, for ET-detected events, due to the time-dependent modulation of antenna beam-pattern related to the Earth’s rotation, a typical sky localization error is at the level of $10^2\text{--}10^3 \text{ deg}^2$. Noting the strong degeneracy between sky localization and luminosity distance, because the polarization angle of a GW signal is dependent on the relative position of the GW source and the detector; such a large sky localization error results in a large uncertainty on polarization, which translates into a large uncertainty on inclination angle and eventually on luminosity distance. Although the majority of GW signals detected by ET have a high SNRs (on the order of $10^2\text{--}10^3$), the typical relative error on the luminosity distance is about 0.1.

Of course, the multi-band GW cosmology is only meaningful if one can identify the common origin of a binary from both frequency bands. Fortunately, this can be achieved thanks to the excellent parameter recovery ability in either frequency band. Two binary black hole signals that share highly consistent merging time ($\Delta t_c \lesssim 1 \text{ s}$), location ($\Delta\Omega \lesssim 1 \text{ deg}^2$), mass ($\Delta M_z/M_z \sim 10^{-7}$), and distance ($\Delta D_L/D_L \sim 10^{-1}$) can be easily identified as the same binary [83]. Even in the pessimistic scenario that the SNR in TianQin band is too weak for independent detection, the archival search methods [102, 103, 106] can be used to find the signal. Searching for archive data triggered by ET detections is a very practical way to achieve multi-band identification.

One remarkable conclusion we can draw from Figure 4 is that the multi-band GW detection can significantly improve the estimation precision of the luminosity distance. Accu-

Table 1 Total detection rate of the SBBHs with $t_c < 20 \text{ yr}$ over the entire observation time that based on the “Power Law+Peak” SBBH population model for five detector configurations: TianQin, TianQin I+II, LISA, TianQin+LISA, and TianQin I+II+LISA

SNR threshold	Total detection rate				
	TianQin	TianQin I+II	LISA	TianQin+LISA	TianQin I+II+LISA
$\rho \geq 5$	$44.2^{+43.1}_{-21.1}$	$111.6^{+108.1}_{-53.3}$	$74.2^{+70.3}_{-36.2}$	$155.9^{+147.4}_{-75.7}$	$245.8^{+234.9}_{-120.1}$
$\rho \geq 8$	$10.8^{+10.1}_{-5.5}$	$28.4^{+26.0}_{-14.9}$	$16.8^{+16.7}_{-8.2}$	$38.3^{+36.1}_{-19.4}$	$63.8^{+58.7}_{-32.7}$
$\rho \geq 12^{\text{a)}$	$3.0^{+3.1}_{-1.4}$	$7.8^{+7.8}_{-3.6}$	$4.6^{+4.6}_{-1.9}$	$10.6^{+9.9}_{-5.2}$	$17.5^{+17.6}_{-8.5}$

a) A conservative SNR threshold [83].

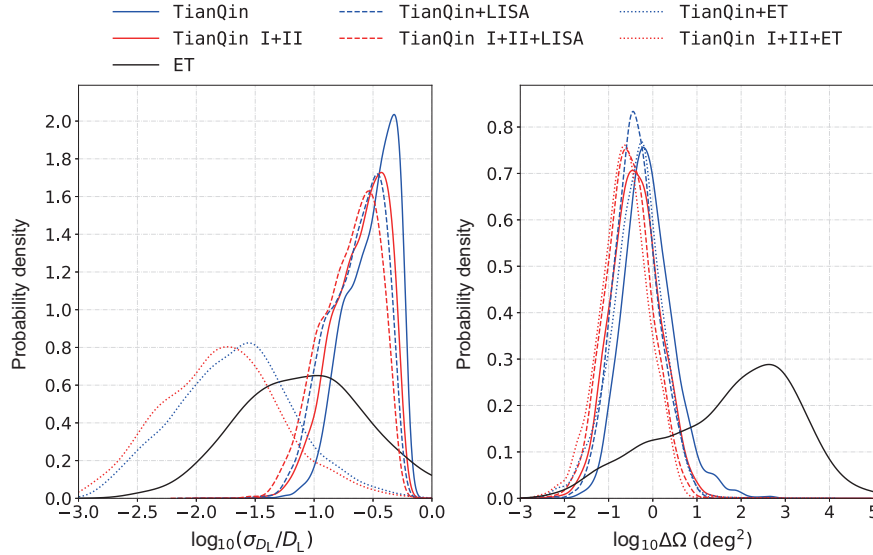


Figure 4 (Color online) Spatial localization error distribution of TianQin (solid blue line), TianQin I+II (solid red line), TianQin+LISA (dashed blue line), TianQin I+II+LISA (dashed red line), TianQin+ET (dotted blue line), TianQin I+II+ET (dotted red line), and ET (solid black line).

rate GW detection from space-borne detectors can provide very precise sky localization, breaking the degeneracy between sky localization and luminosity distance for ground-based detectors. The relative error on luminosity distance can be improved by one order of magnitude compared with TianQin/LISA and by half an order of magnitude compared with ET.

3.3 Statistical redshift

The spatial localization information of the GW source cannot be directly used to select candidate host galaxies of the GW source. The possible range of luminosity distance $[D_L^-, D_L^+] \equiv [(\bar{D}_L - 2\sigma_{D_L}), (\bar{D}_L + 2\sigma_{D_L})]$ (where \bar{D}_L is the mean value) needs to be converted into the possible range of redshift $[z^-, z^+]$ first. The candidate host galaxies are then selected from the survey galaxy catalog using the redshift-space error box. This conversion depends on both a specific cosmological model and the prior of the corresponding cosmological parameters. We convert the luminosity distance range into the redshift possible range under the standard Λ CDM model, with the prior of $H_0 \in U[30, 120] \text{ km s}^{-1} \text{ Mpc}^{-1}$ and $\Omega_M \in U[0.04, 0.6]$. The conversion relation is given by

$$D_L^- = c(1 + z^-) \int_0^{z^-} \frac{1}{H^-(z')} dz', \quad (20a)$$

$$D_L^+ = c(1 + z^+) \int_0^{z^+} \frac{1}{H^+(z')} dz', \quad (20b)$$

where $H^-(z)$ and $H^+(z)$ are the specific Hubble parameter realizations that minimize and maximize eq. (1) within the prior of both H_0 and Ω_M .

In our simulation, we obtain the candidate host galaxies of the GW source from the GWENS catalog. To properly account for the redshift uncertainty, we consider two factors: (1) The redshift information of galaxy in the catalog is almost all photo- z , including non-negligible photo- z error Δz_{photo} ; (2) due to the peculiar velocity of galaxies, the observed spectroscopic redshift z_{obs} is different from the cosmological redshift z , and we denote this redshift error $\Delta z_{\text{pv}} \equiv |z_{\text{obs}} - z|$. In general, $\Delta z_{\text{photo}} \gg \Delta z_{\text{pv}}$, so the final boundary of the redshift of candidate host galaxies is defined as $[z_{\min}, z_{\max}] = [(z^- - \Delta z_{\text{photo}}), (z^+ + \Delta z_{\text{photo}})]$. The final spatial localization error box of candidate host galaxies is defined by $4\Delta\Omega \times [z_{\min}, z_{\max}]$ (the factor of 4 corresponds to the 2σ confidence level for the GW sky localization). For a small number of galaxies with spectroscopic redshift, we discard Δz_{photo} and approximate $\Delta z_{\text{pv}} \approx (1 + z_{\text{obs}})\langle v_p \rangle/c$, assuming $\langle v_p \rangle = 500 \text{ km/s}$ [169]. The impact of peculiar velocities and their reconstruction on the estimation of H_0 has been studied in refs. [169–172], and it is possible to eliminate the redshift error Δz_{pv} for nearby galaxies.

To obtain the statistical redshift distributions of GW sources, for each galaxy in the localization error box, we adopt the following two methods:

- fiducial method: assigning equal weight regardless of its position and luminosity;
- weighted method: assigning a weight that accounts for both its positional and luminosity-related information.

When the sky localization from GW detection is described by a covariance matrix $\Sigma_{\alpha\delta}$, the positional weight of a galaxy at location (α_j, δ_j) is defined as $W_{\text{posi}} \propto \exp\left\{-\frac{1}{2} \left[(\alpha_j - \bar{\alpha}, \delta_j - \bar{\delta}) \Sigma_{\alpha\delta}^{-1} (\alpha_j - \bar{\alpha}, \delta_j - \bar{\delta})^T \right]\right\}$, where $(\bar{\alpha}, \bar{\delta})$

are the best measured values of the sky localization. Meanwhile, we apply a luminosity-related weight corresponding to total stellar mass of the galaxy, which is derived using multi-band photometric information through the Le Phare software (see sect. 2.4 for details).

Figure 5 illustrates an example localization of a SBBH GW signal and the impact of different weighting methods as well as redshift (photometric or spectroscopic) on the final redshift estimation of the SBBH. While the sky localization of GW source is insufficiently precise to uniquely identify the host galaxy in the absence of an EM counterpart; more accurate sky localization can eliminate the interference of many polluting galaxies. The left panel shows the advantage of the more accurate sky localization of TianQin I+II over TianQin in selecting the galaxies; the middle panels show the different distributions of the statistical redshifts for the two detector configurations. One can conclude that with fewer candidate host galaxies, the true host galaxy's redshift becomes more significant. Additionally, the distribution of redshift determined by photometric data appears to be more smooth due to large photo-z error, whereas the distribution determined by spectroscopic data shows larger fluctuations, implying a greater potential for constraining the Hubble constant. Notably, because the quality of the statistical redshift distribu-

tion for the host galaxy is mainly dependent on the spatial localization precision provided by the GW detection, we do not repeat the above illustration for other configurations where the sky localization is not significantly different.

It is slightly counter-intuitive that improved sky localization would result in a worse redshift estimate. This is because the photo-z estimate for any single galaxy is usually accompanied by a sizeable random error. When the GW signal is localized to a larger area, it involves a greater number of galaxies, and the intrinsic clustering of galaxies effectively averages out the random error. On the other hand, such averaging is less effective for more accurate sky localization. However, we anticipate that future detections will trigger an interest in a comprehensive survey of galaxies within the GW localization error box. Therefore, we expect that for events with a spatial resolution of less than $\Delta\Omega < 0.1 \text{ deg}^2$, spectroscopic redshift will be available for galaxies with an apparent magnitude $m_{\text{app}} \leq +21 \text{ mag}$ [173]. In practice, we simply adopt the median value of the photo-z as the “true value” of the spectroscopic redshift.

4 Results

To extract the Hubble constant from the dark standard sirens,

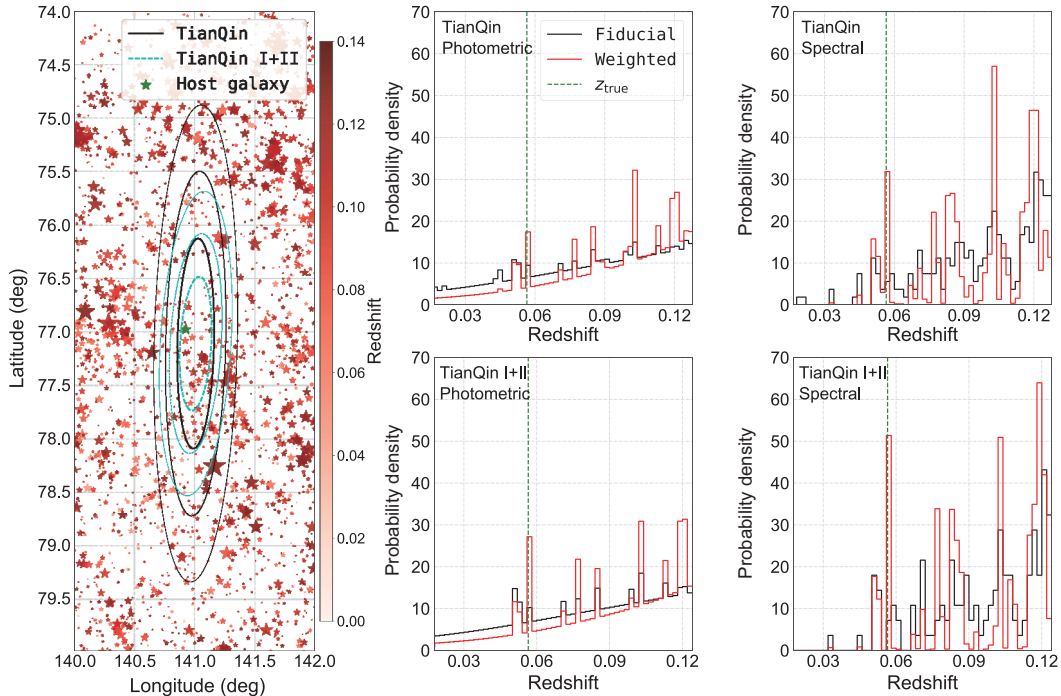


Figure 5 (Color online) Sky localization and statistical redshift distribution of an example SBBH inspiral. The left panel shows sky localizations of TianQin (solid black contour lines) and TianQin I+II (dashed cyan contour lines), as well as a scatter plot of galaxies within the catalog. The green star labels the real host galaxy; the shade of the star represents its redshift, and the size of the star represents its luminosity-related weight. The center panels show the statistical photo-z of TianQin (top) and TianQin I+II (bottom), respectively, using two different statistical redshift estimations with both the fiducial method (black histograms) and the weighted method (red histograms), and the vertical green dashed line represents the true redshift of the GW source. The right panels show the same as the center panels but with spectroscopic galaxy redshifts.

we use a Markov chain Monte Carlo (MCMC) algorithm—emcee package, which is a Python implementation of an affine-invariant MCMC ensemble sampler [174, 175]. In Figure 6, we illustrate how to estimate cosmological parameters using the SBBH GW detections of TianQin I+II. We demonstrate that although a single event may suffer from large uncertainties due to its inability to identify the host galaxy, but a number of events can cancel out the random error and result in a more precise estimate of the Hubble constant.

Because of the uncertainty related to the luminosity distance, the redshift (Δz_{photo} and Δz_{pv}), and the cosmological model, a single GW event is frequently associated with a large number of galaxies with a wide range of redshifts (see eqs. (20a) and (20b)), which are shown as the horizontally distributed dots in Figure 6. After constraining cosmological parameters, the redshift range of candidate host galaxies of the GW source will be considerably reduced, which is referred to as posterior redshift. The candidate host galaxies within the posterior redshift range ultimately determine the precision with which cosmological parameters can be estimated. The other candidate host galaxies outside the posterior redshift are just interference sources, and we cannot exclude them when the cosmological parameters are not constrained.

The results of constraints on H_0 using SBBH GW signals are shown in this section for different detector configurations, including TianQin, TianQin I+II, TianQin+LISA, TianQin I+II+LISA, TianQin+ET, and TianQin I+II+ET. To alleviate the random effect of random realization, we repeat the calculation on 48 random realizations with different random seeds

for each configuration and the two weighting methods. Furthermore, when reporting the constraining on H_0 , the result is marginalized over Ω_M instead of being fixed at a specific Ω_M value.

4.1 TianQin and TianQin I+II

The current studies of the population properties of SBBH merger events observed by LIGO and Virgo have revealed a large uncertainty in the merger rate of SBBHs [20, 25, 160, 162], which also results in large uncertainty in the prediction of the detection rate of GW events derived from SBBHs. We studied the variation of the constraint precision of H_0 with the number of GW events in a range of 6 to 120 events to avoid the influence of the detection rate of GW events on the constraint precision of H_0 and fully display the potential of detectors. The constraints on H_0 for TianQin and TanQin I+II are shown in Figure 7. The uncertainty of H_0 shrinks as the number of detected GW events increases. In comparison to the fiducial method, the weighted method can improve the constraining precision of H_0 by a factor of about 2.

TianQin can detect approximately 11 SBBH GW events over 5 years of operation (as illustrated in Table 1), with which one can constrain H_0 to a precision of approximately 36.8% using the fiducial method and approximately 30.9% using the weighted method, respectively. Due to the small number of GW events, the constraints on cosmological parameters are very imprecise. A typical constraint result of the parameters h ($h \equiv \frac{H_0}{100 \text{ km s}^{-1} \text{ Mpc}^{-1}}$) and Ω_M from TianQin using the weighted method is shown in the left plot of

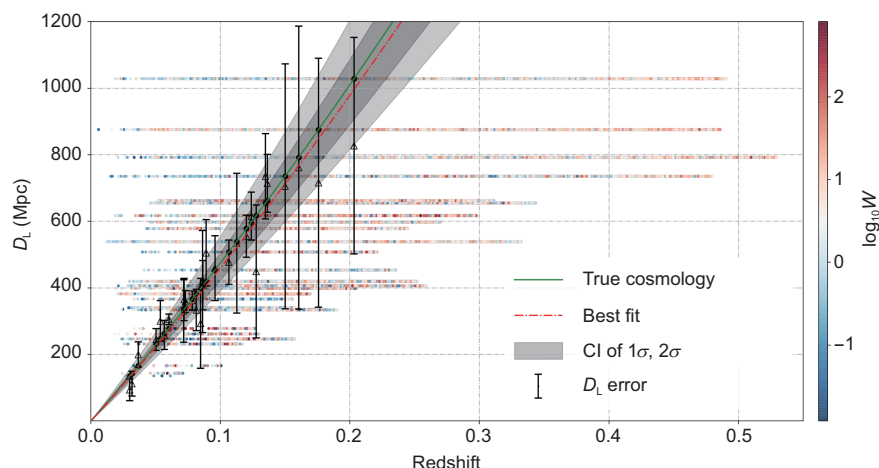


Figure 6 (Color online) Example of fitting the “ D_L-z relation” based on the dark standard siren observations of TianQin I+II. The solid green line represents injected cosmological parameters H_0 and Ω_M . The dotted-dashed red line represents the most probable cosmology, while the two shaded areas represent confidence intervals of 68.27% (1σ) and 95.45% (2σ), respectively. The black error bars represent measurement errors in determining the luminosity distance to GW sources. The median hollow black triangles in each error bar represent the mean of the D_L measurement with random statistical deviation, while the solid black dot represents the true value of D_L . The horizontal colored dots represent the redshift of selected galaxies for that particular source. The color hues from blue to red show the logarithms of the total weights of galaxies, and we assigned a value to the D_L of each candidate host galaxy equal to the true D_L of the GW source.

Figure 8.

The constraint on H_0 with TianQin I+II is tighter than that with TianQin, as shown in Figure 7. Given the same number of GW events and the weighting method of candidate host galaxies, TianQin I+II can significantly improve the constraint of H_0 . This improvement is mainly due to the more accurate spatial localization provided by TianQin I+II, as shown in Figure 4. Using the fiducial method and the weighted method, approximately 28 GW events are ex-

pected to be detected by TianQin I+II, and the precision of H_0 is expected to be approximately 26.3% and 14.4%, respectively. A typical cosmological parameter estimation using the weighted method for TianQin I+II is shown in the right plot of Figure 8. The non-Gaussian tail of the posterior probability distribution of H_0 becomes shorter as the rate of GW detection increases and the spatial localization of GW sources becomes more precise. Additionally, when using SBBH GW events, either for TianQin or TianQin I+II,

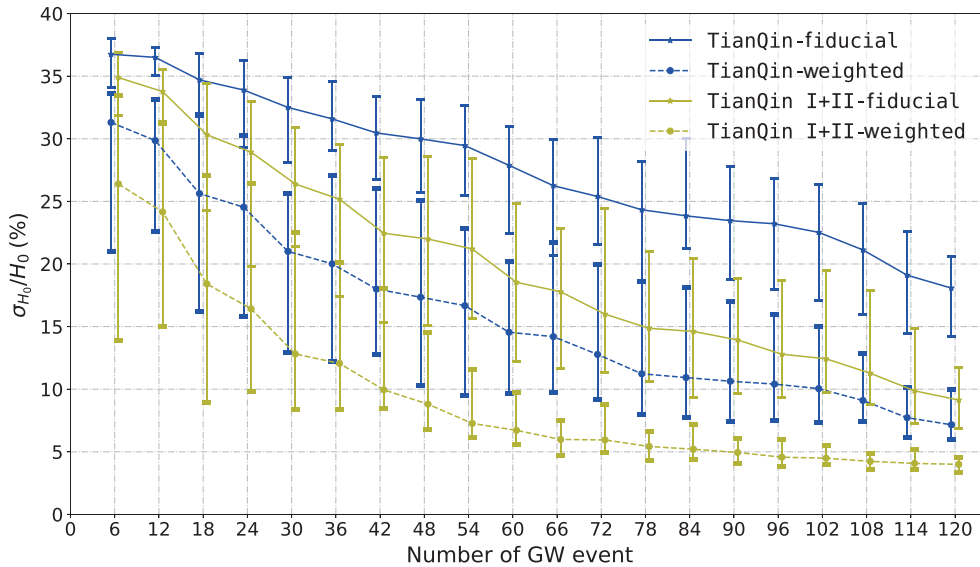


Figure 7 (Color online) Dependence of constraint precision of H_0 on the numbers of GW events for TianQin (blue) and TianQin I+II (yellow). The fiducial method and the weighted method are shown in solid and dashed lines, respectively. Each error bar represents a 68.27% interval from 48 independent simulations. The lines have been slightly shifted to improve the visual presentation.

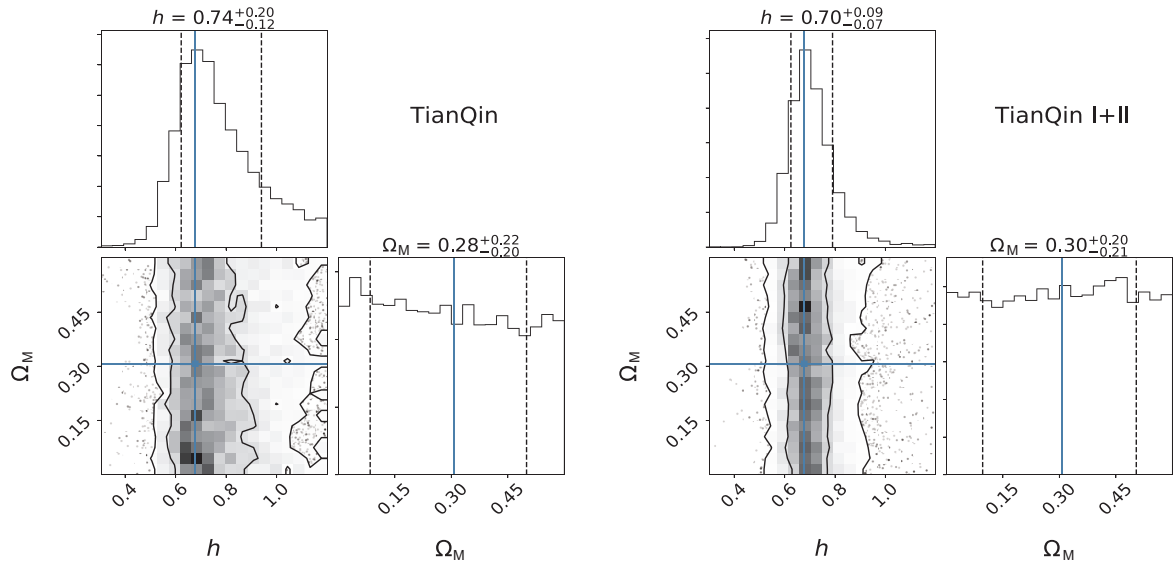


Figure 8 (Color online) Example posterior probabilities of the parameters h and Ω_M calculated using the weighted method for TianQin (left) and TianQin I+II (right). In each plot, the lower left panel shows the joint posterior probability of h and Ω_M , with the contours representing confidence levels of 1σ (68.27%) and 2σ (95.45%), respectively; the upper and right panels show the marginalized posterior distribution of the same parameters, with the dashed lines indicating a 1σ credible interval. In each panel, the solid cyan lines mark the true values of the parameters.

there are no effective constraints on Ω_M parameter. It is worth noting that the precision of H_0 estimation with TianQin using the weighted method is higher than that obtained using the fiducial method with TianQin I+II, indicating that in comparison to improved spatial localization, the more accurate weighting method has a larger impact on H_0 estimation.

4.2 Multi-detector network of TianQin and LISA

We then analyze scenarios in which LISA is added to the de-

tector network. In Figure 9, we show the dependence of the precision of H_0 versus detection numbers, assuming TianQin+LISA and TianQin I+II+LISA. Again we observe that increasing the number of detections results in a more precise H_0 measurement. In Figure 10, we give a representative joint posterior probability of h and Ω_M using the weighted method under the expected total detection rates (see Table 1 for details). We notice that TianQin+LISA has very similar constraining power to TianQin I+II because the two detection configurations have very similar localization precisions

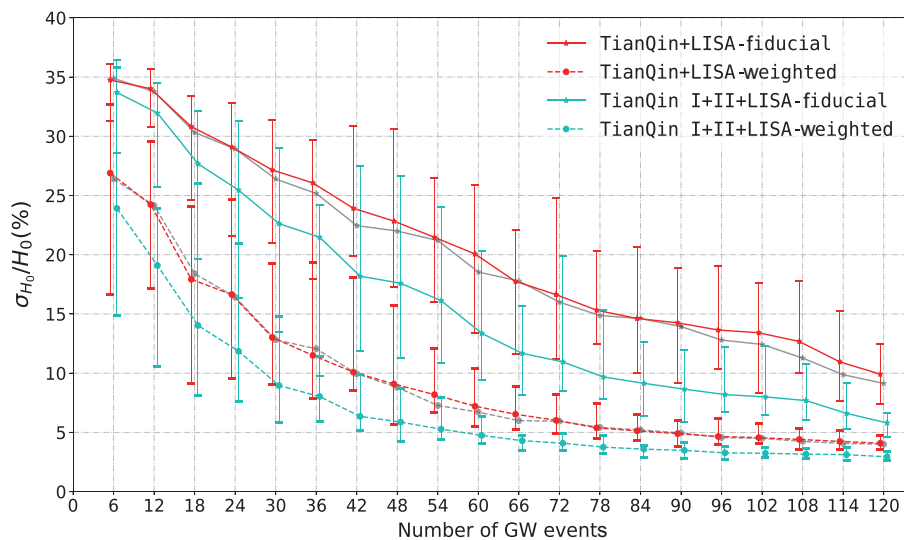


Figure 9 (Color online) Dependence of constraint precision of H_0 on the numbers of GW events for TianQin+LISA (red) and TianQin I+II+LISA (cyan). The fiducial method and the weighted method are shown in solid and dashed lines, respectively. Each error bar represents a 68.27% interval generated by 48 independent simulations. For comparison, similar results for TianQin I+II (gray) are also shown. The lines have been slightly shifted to improve the visual presentation.

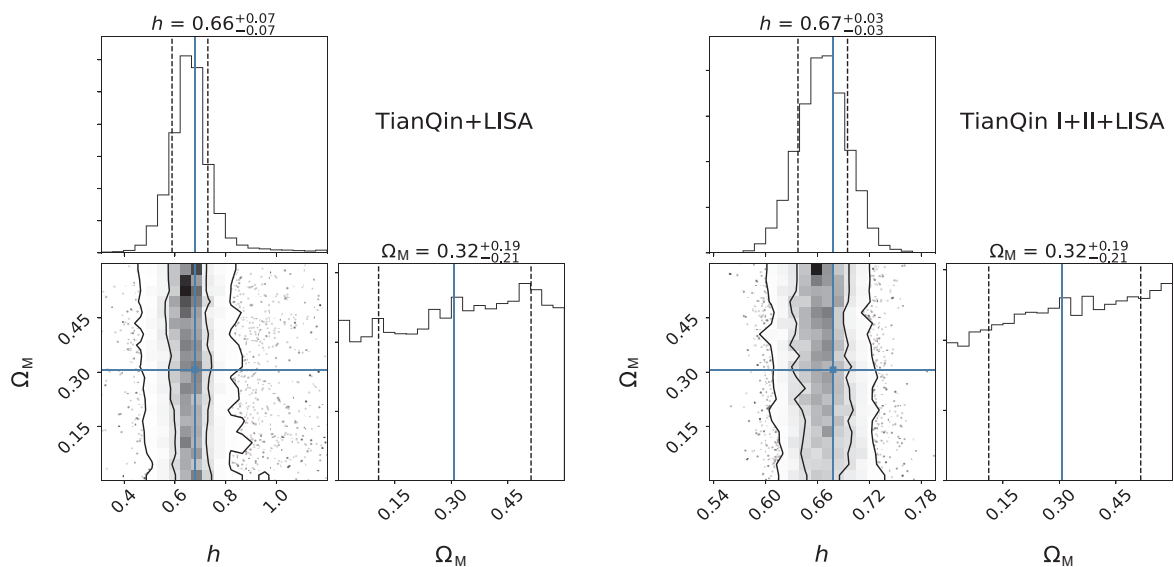


Figure 10 (Color online) Example posterior probabilities of the parameters h and Ω_M calculated using the weighted method for TianQin+LISA (left) and TianQin I+II+LISA (right). Each plot represents the joint posterior probability of h and Ω_M , with contours representing confidence levels of 1σ (68.27%) and 2σ (95.45%), respectively; the upper show the marginalized posterior distribution of the same parameters, with the dashed lines representing the 1σ credible interval. In each panel, the solid cyan lines mark the true values of the parameters.

(Figure 4). Meanwhile, TianQin I+II+LISA can reduce uncertainty on H_0 by half as a result of improved localization. On the other hand, neither of the two detector network configurations, imposes any meaningful constraint on Ω_M .

For TianQin+LISA (TianQin I+II+LISA), about 38 (64) GW events are expected to be detected, and the precision of H_0 can be constrained to approximately 25.2% (12.2%) and approximately 11.6% (4.1%) by using the fiducial method and the weighted method, respectively. Similar to the case of TianQin and TianQin I+II, the constraint of H_0 by TianQin+LISA using the weighted method is stronger than that by TianQin I+II+LISA using the fiducial method.

Space-borne GW detectors/networks have excellent sky localizing capabilities, which enables the constraints on the Hubble constant through the observation of SBBH inspirals. However, such SBBH inspiral GW signals are relatively quieter; the relatively lower SNR leads to a larger uncertainty on luminosity distance, $\sigma_{D_L}/D_L \gtrsim 0.1$. This fact limits the expected precision of H_0 from the SBBH inspiral observation with space-borne detectors.

4.3 Multi-band detection with TianQin and ET

A multi-band GW observation of SBBHs can significantly improve the constraining on the Hubble constant under the dark standard siren scenario since the multi-band observation combines advantages of both space-borne and ground-based detectors. Space-borne GW detectors can provide accurate sky localization, while ground-based detectors' high SNR enables more precise luminosity distance estimation. This combination results in a smaller localization error box that is

less susceptible to contamination from neighbouring galaxies, resulting in a more precise estimation of the redshift.

In Figure 11, we present the dependence of constraint precision of H_0 versus different detection numbers, under the multi-band GW detector networks TianQin+ET and TianQin I+II+ET. Notably, the TianQin I+II lines (gray) approximate a power-law relationship, while the lines for multi-band networks indicate a saturation from relative uncertainties around 1.8%, which also corresponds to a turning point for the trend of the lines, respectively. We observe that the multi-band network can quickly increase the precision of H_0 as more events are observed, but after the turning point, the precision improves only by $1/\sqrt{N}$, where N is the number of GW events. Moreover, the precision is hard to reach the level of 1% even after 100 GW events are detected. Additionally, we notice that when adopting the weighted method, better precision leads to a quicker approach to saturation, which occurs in around 24 events for the TianQin I+II+ET network.

For TianQin+ET, about 44 GW events are expected to be detected via multiple band observation (as illustrated in Table 1), and the precision of H_0 can be constrained to approximately 4.7% and approximately 1.5% by using the fiducial method and the weighted method, respectively. Moreover, if TianQin I+II+ET is realized, approximately 112 GW events can be detected using multi-band observations in the optimistic case, and the precision of H_0 can be constrained to $\sim 1\%$, using either the fiducial method (about 1.3%) or the weighted method (about 1.1%). Constraining H_0 to a precision of 1% would be very exciting as it has the potential to shed light on the Hubble tension .

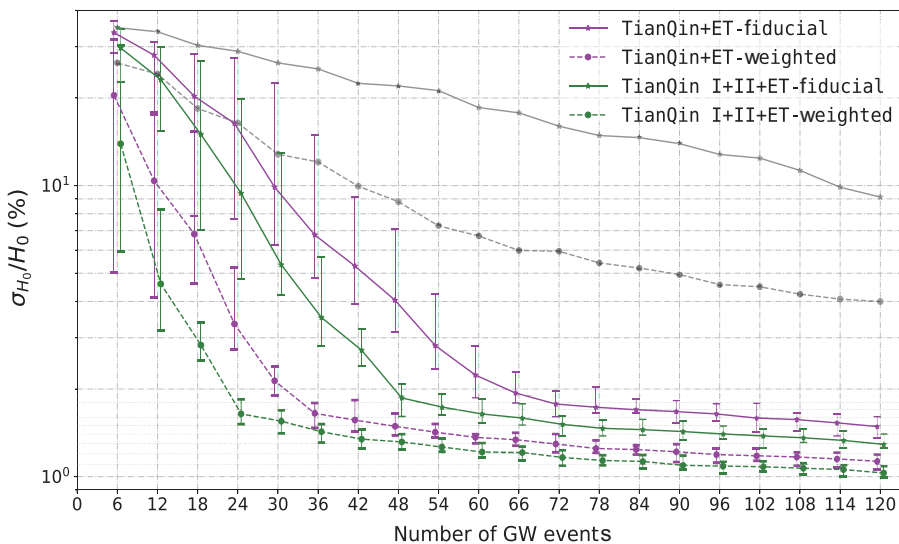


Figure 11 (Color online) Dependence of constraint precision of H_0 on the numbers of GW events for TianQin+ET (magenta) and TianQin I+II+LISA (green). The fiducial method and the weighted method are shown in solid and dashed lines, respectively. Each error bar represents a 68.27% interval from 48 independent simulations. Comparable results for TianQin I+II (gray) are also provided. The lines have been slightly shifted to improve the visual presentation.

The typical constraints on h and Ω_M using the weighted method for the multi-band networks are shown in Figure 12. The introduction of multi-band GW observation can greatly enhance the constraining power on the cosmological parameter Ω_M . While the fiducial method does not deliver significant and robust estimation, the weighted method can constrain Ω_M to a precision of 0.13, or equivalently 42% for relative uncertainty, with the TianQin I+II+ET network.

5 Discussions

5.1 Important role of spectroscopic redshift

Considering that the sky localization error of almost all GW sources is less than 10 deg^2 , it may be possible to use current or future spectroscopic observation facilities, such as the Large Sky Area Multi-Object Fiber Spectroscopic Telescope [176-178], the Dark Energy Spectroscopic Instrument [179], the 4-meter Multi-Object Spectroscopic Telescope (4MOST) [180], the TAIPAN [181], the Chinese Space Station Telescope [173], the James Webb Space Telescope [182, 183], and the Wide-Field Infrared Survey Telescope [184, 185], to perform galaxy survey and provide accurate estimations of redshifts for the galaxies located in the error box. In this section, we investigate to what extent a catalog of galaxies with spectroscopic redshifts can improve the constraint precision of H_0 . Table 2 summarizes the constraint precision of H_0 under various detector configurations and under two assumptions that the survey galaxy catalog with photo-z and with

assumed spectroscopic redshift, respectively.

We observe that the constraint precision of H_0 is quite low for TianQin. This is because the expected detection rate is low; the detected events are insufficient to suppress random fluctuations, and so the effect of spectroscopic redshift is not significant. However, for a network of detectors, one might anticipate a greater number of detected GW events, which emphasizes the uncertainty associated with the galaxy redshift measurement. We observe that employing spectroscopic redshift can significantly improve the precision of H_0 by a factor of 2. However, for TianQin I+II+ET, the saturation described in sect. 4.3 allows for extremely exact estimation of H_0 even without the spectroscopic redshift. But still, by using the weighted method and the spectroscopic redshift, one can expect the H_0 to be constrained to a level better than 1%.

5.2 Information gained from multiple band photometry information

The use of multi-band luminosity can aid in our comprehension of the redshift information. In this paper, we quantify the role of the multi-band luminosity information in this process. For different weighting scenarios, we calculate the *information gain* of statistical redshift distributions on top of the prior distribution. The information gain is defined as [186]:

$$\mathcal{H} = \int p(z|d_{\text{GW}}, d_{\text{survey}}, \mathbf{H}, I) \log_2 \left[\frac{p(z|d_{\text{GW}}, d_{\text{survey}}, \mathbf{H}, I)}{p_c(z|\mathbf{H}, I)} \right] dz, \quad (21)$$

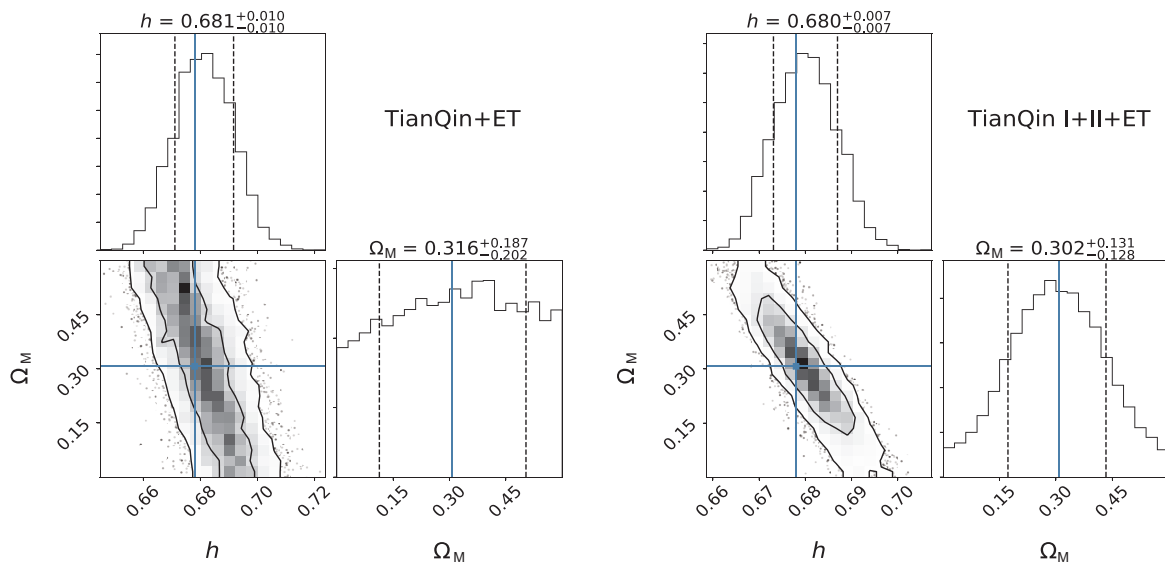


Figure 12 (Color online) Example posterior probabilities of the parameters h and Ω_M calculated using the weighted method for TianQin+ET (left) and TianQin I+II+ET (right). In each plot, the lower left panel shows the joint posterior probability of h and Ω_M , with the contours representing confidence levels of 1σ (68.27%) and 2σ (95.45%), respectively; the upper and right panels show the marginalized posterior distribution of the same parameters, with the dashed lines indicating a 1σ credible interval. In each panel, the solid cyan lines mark the true values of the parameters.

where $p(z|d_{\text{GW}}, d_{\text{survey}}, \mathbf{H}, I)$ represents the posterior of redshift for candidate host galaxies of GW sources, d_{survey} represents data of galaxy survey, and $p_c(z|\mathbf{H}, I)$ is the prior distribution on redshift, which is defined by eq. (11).

We illustrate the information gains on statistical redshift in Figure 13, for four weighting methods: (1) the fiducial method, (2) single-band luminosity weighting method, (3) multiple band luminosities weighting method, and (4) position plus multi-band luminosity weighting method. A total of

2000 mock GW events are used. As can be shown, all methods yield a greater information gain when the localization error is smaller. With more information (in terms of luminosity and position), more information about statistical redshift can be gained. The peak of the marginalized distribution (shown on the top panel) demonstrates that for the four methods, each step provides an information gain increase of roughly 0.1 bits. Moreover, the information gain from the single-band luminosity weighting method is approximately

Table 2 Expected constraint precision of H_0 under six detector configures, assuming the survey galaxy catalog with photo-z and with spectroscopic redshift. The error represents 68.27% confidence interval

Network configuration	Constraint precision σ_{H_0}/H_0 (%)			
	Using photo-z catalog		Using spectroscopic redshift catalog	
	Fiducial method	Weighted method	Fiducial method	Weighted method
TianQin	$36.8^{+1.7}_{-1.8}$	$30.9^{+5.1}_{-5.1}$	$29.7^{+5.4}_{-6.2}$	$22.2^{+8.3}_{-9.8}$
TianQin I+II	$26.3^{+5.9}_{-6.9}$	$14.4^{+9.4}_{-7.6}$	$15.1^{+9.4}_{-6.9}$	$7.9^{+2.9}_{-3.2}$
TianQin+LISA	$25.2^{+6.4}_{-7.6}$	$11.6^{+8.2}_{-6.4}$	$12.4^{+6.2}_{-5.4}$	$6.4^{+1.6}_{-2.4}$
TianQin I+II+LISA	$12.2^{+5.3}_{-5.3}$	$4.1^{+0.8}_{-0.8}$	$5.7^{+1.5}_{-2.0}$	$3.3^{+0.7}_{-0.7}$
TianQin+ET	$4.67^{+1.80}_{-1.60}$	$1.51^{+0.13}_{-0.13}$	$2.10^{+0.25}_{-0.63}$	$1.32^{+0.10}_{-0.09}$
TianQin I+II+ET	$1.32^{+0.07}_{-0.09}$	$1.05^{+0.05}_{-0.06}$	$1.08^{+0.10}_{-0.09}$	$0.95^{+0.08}_{-0.08}$

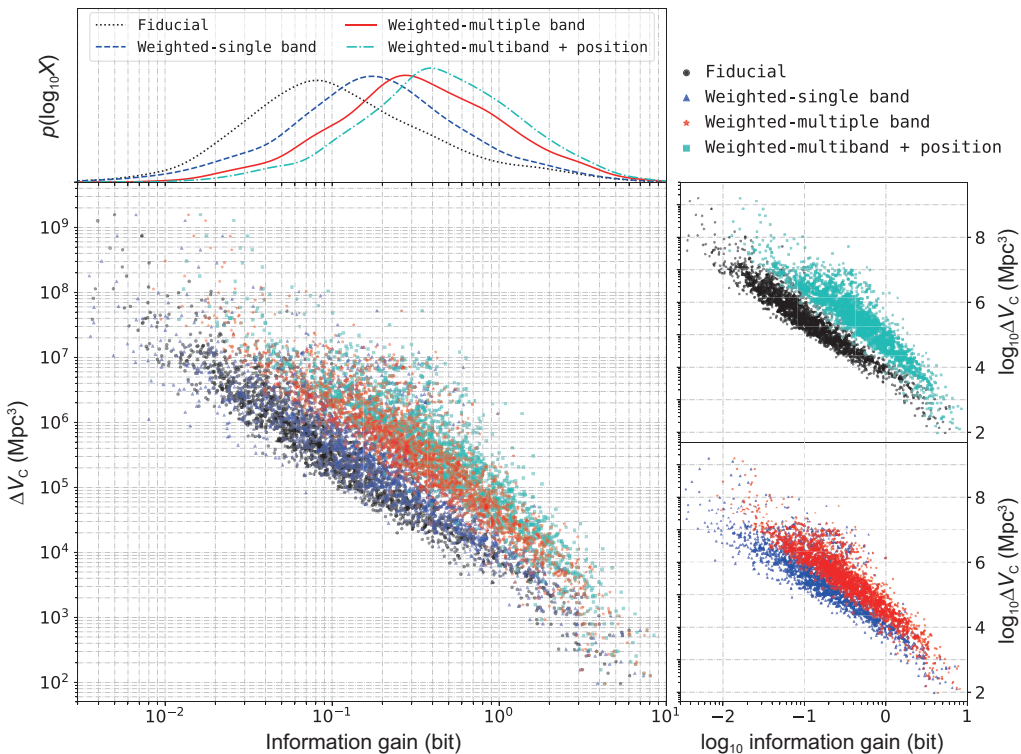


Figure 13 (Color online) Distribution of statistical redshift information gains for various weighting methods. The black, blue, red, and cyan dots or lines represent the results obtained by the fiducial method, single-band luminosity weighting, multiple band luminosities weighting, and the position plus multi-band luminosity weighting methods, respectively. This figure contains 2000 mock GW events detected from TianQin. The top panel shows the distribution of information gains obtained using these four methods, the bottom left panel shows the scatter distribution of information gain-localization co-moving volume of candidate host galaxies (ΔV_C), the right panels decompose the scatters for better distinction.

the same for any of the five bands of *ugriz*. In most cases, the weighting method of using both location and multi-band luminosities can yield an information gain of as high as about 0.5 bits.

5.3 Potential to address the Hubble tension

Astronomers are puzzled by the Hubble tension, which describes the inconsistency between the two typical Hubble constant measurement methods, reported as (74.03 ± 1.42) km s $^{-1}$ Mpc $^{-1}$ from SNe Ia observations [7] (also see ref. [9]) and (67.4 ± 0.5) km s $^{-1}$ Mpc $^{-1}$ from the *Planck* CMB anisotropies measurements [3]. Both methods have remarkable accuracies of approximately 1.9% and 0.7%, respectively. GW cosmology with dark standard sirens provides a fascinating new means of potentially explaining or resolving the Hubble tension, as it is expected to be much less impacted by systematic errors. However, an equally accurate measurement would be required to achieve so. With the TianQin detectors, even in the most optimal scenario where we assume TianQin I+II with the weighted method and a galaxy catalog with spectroscopic redshift, the estimated precision of H_0 can only reach 7.9%. When LISA is included, the precision can reach the level of 3.3%.

On the other hand, a multi-band GW detector network has a very prominent potential to estimate H_0 accurately. One can expect an H_0 precision of 1.51% and 1.05% for TianQin+ET and TianQin I+II+ET, respectively, which is very promising for addressing, or at the very least, shedding light on the nature of the Hubble tension.

According to some studies suggest that the multi-detector GW detections of MBHB mergers can also achieve precision close to (or even better than) 1% for H_0 measurement. This level of precision is typically facilitated by the fact that the MBHB mergers may be registered with a very high SNR using space-borne GW missions [76, 78, 85, 187-189]. Meanwhile, since MBHB mergers may be detected at a very long distance, they may also be used to recover additional cosmological parameters in addition to H_0 . However, the precision of H_0 with MBHB detections is highly sensitive to the detection of neighboring events, which usually have a very low detection rate; the high precision is not guaranteed [92, 93]. On the other hand, the higher detection rate of SBBHs indicates a highly likely prospect of using their inspiral GW signals to constrain H_0 with high precision.

5.4 P-P plot check

To compensate for the selection effect of galaxies observations, we adopt a correction factor in eq. (12) with the goal of obtaining an unbiased estimate of the Hubble constant. We

want to examine whether the conclusion is indeed unbiased, using both the weighted method and the fiducial method. To do this, we perform a series of *P-P* plots to ensure consistency, as shown in Figure 14. The horizontal axis shows the credible level, while the vertical axis shows the fraction of simulations in which the true parameters are located within a certain credible interval. For a fully consistent method, we expect the *P-P* plot to be alongside the diagonal line, with some degree of random fluctuations. For a more straightforward comparison, we perform Kolmogorov-Smirnov tests for different lines versus the diagonal line and present the calculated *p*-value in Table 3, with a larger *p*-value representing better consistency.

In the left panel, assuming that just photo-z is available for the galaxies, the majority of the solid lines (or the fiducial method) deviate significantly from the diagonal, with a general pessimistic tendency. This is because the posterior probability of the cosmological parameters using the fiducial method does not gain sufficient redshift information from a large number of candidate host galaxies, resulting in a large credible interval, but the true value has most likely already been enclosed. We observe, on the other hand, that the result from the weighted method (dashed lines) is more consistent with the diagonal line, fluctuating well within the 3σ confidence interval, which indicates a successful implementation of an unbiased estimator for the Hubble constant.

If galaxies have spectroscopic redshifts, both methods' *P-P* plots are statistically consistent with the diagonal for all configurations. This finding emphasizes the importance of accurate measurement of galaxy redshifts in estimating the Hubble constant.

5.5 Effect of eccentricity on multi-band GW detection

In this work, we focus on GW sources with very small eccentricities ($e_0 = 0.01$ at 0.01 Hz). This is a reasonable assumption for binary black holes generated via an isolated binary channel, as the GW radiation is expected to circularize the orbit. However, if the SBBHs have a dynamical origin, they may retain higher eccentricities in the millihertz range [190, 191], which may affect the multi-band GW detection [192-194]. Indeed, the observations of GW190521 by LIGO and Virgo may suggest such a possibility [23, 195, 196]. For extreme eccentricities, the GW signals in the millihertz band may fall below the sensitivity of space-borne GW detectors [193]. Fortunately, the majority of SBBHs are not expected to be associated with extreme eccentricities [166, 197], and the general conclusion of our study should not be altered by the inclusion of eccentricities.

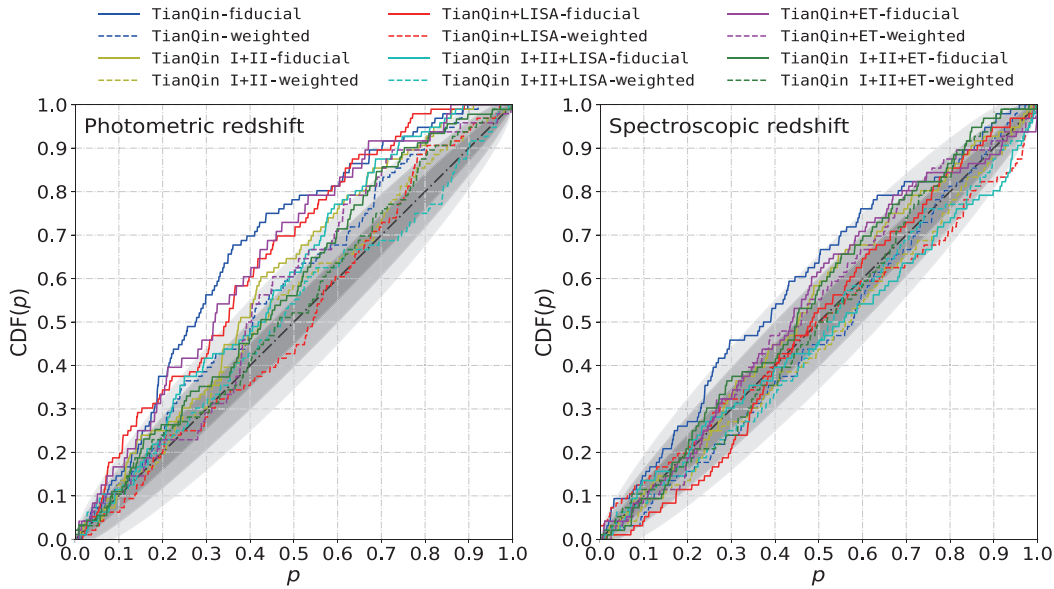


Figure 14 (Color online) P - P plot over 96 independent simulations on the estimation of the Hubble constant for various detector configurations. The p on the x axis is the credible level, and the $CDF(p)$ (cumulative distribution function, CDF) on the y axis is the fraction of simulations with true parameters within the credible interval. Results with different configurations are shown in different colors, with the fiducial method, the weighted method, and the diagonal line shown in solid, dashed, and dotted-dashed lines, respectively. Different gray shadows represent 1σ , 2σ , and 3σ confidence intervals, respectively. The left panel makes the assumption that galaxies have photo- z whereas the right panel makes the assumption that spectroscopic redshift is available.

Table 3 Meta p -value of the distribution of H_0 estimations obtained from multiple independent simulations under various detector configurations, in comparison to an expected uniform distribution over $[0, 1]$. The null hypothesis is set so that the two distributions are consistent; therefore, a p -value less than 0.05 indicates that the simulation results deviate significantly from the ideal result

Detector configuration	p -value			
	Using photo- z catalog		Using spectroscopic redshift catalog	
	Fiducial method	Weighted method	Fiducial method	Weighted method
TianQin	5.6×10^{-9}	0.0756	9.8×10^{-3}	0.3756
TianQin I+II	3.8×10^{-3}	0.2511	0.1774	0.5081
TianQin+LISA	2.3×10^{-5}	0.2513	0.2026	0.2419
TianQin I+II+LISA	1.9×10^{-3}	0.6767	0.1549	0.4871
TianQin+ET	2.6×10^{-3}	0.1085	0.1030	0.2690
TianQin I+II+ET	0.0209	0.4074	0.2386	0.5599

5.6 Other potential sources of constraint bias on the Hubble constant

Numerous factors can introduce bias into the estimation of the Hubble constant. We describe the potential sources of the bias in this work as follows.

- The detectable SBBH sources are primarily distributed in the $z \lesssim 0.2$, where Hubble's law can be used to approximate the expansion of the Universe. Therefore, in the majority of cases, the model-dependent Ω_M has no effect on the outcomes of our H_0 analysis results. However, a small number of GW events with $z \gtrsim 0.2$ show a certain constraint ability on Ω_M , such as the constraint results of TianQin+ET and TianQin I+II+ET. This implies that the cosmological model

will introduce a bias when using higher redshift SBBH events to constrain H_0 with high precision.

- In the GW event catalog simulation, the GW sources are randomly assigned to one of the galaxies in the survey galaxy catalog. However, the survey galaxy catalog may not contain the true host galaxy of the GW source in the actual H_0 estimation due to the selection effect such as the Malmquist bias. The absence of the true redshift of the GW source in the statistical redshift may also introduce a bias into the estimation of H_0 .

- In the simulation setup, we use the median of photo- z estimation as the true cosmological redshift of the galaxy. However, the actual photo- z measurements have an intrinsic scatter and deviation in relation to the spectroscopic redshifts

[147, 150, 198, 199].

- If some of the detected SBBHs have a primordial black hole genesis, [200-204], the concept of a host galaxy may lose relevance. Furthermore, drawing conclusions based on the assumption that all SBBHs are produced astronomically may be deceptive.

Of course, there are methods to alleviate the bias. For example, the bias of H_0 caused by the cosmological model can be avoided by fitting model-independent high-order expansion of the “ D_L-z relation” [205, 206], or using the model-independent parameter estimation method such as Gaussian processes [62, 66, 207]. The selection effect in the catalog of the galaxy survey can be corrected by conducting a follow-up deeper field galaxy survey triggered by the GW detection [208-210], utilizing both ground-based [211, 212] and space telescopes [173, 184]. By performing a follow-up spectroscopic measurement, the bias introduced by photo- z can be eliminated. Although the possibility of contamination by primordial black holes requires additional investigation, an internal consistency check as introduced in refs. [87, 92] may help in identifying and removing the anomaly.

6 Conclusions and outlook

In this work, we investigate the potential of using SBBH GW events (assuming the “Power Law+Peak” model) observed by space-borne GW detectors as dark standard sirens to constrain the Hubble constant. Several different detection scenarios are considered, for instance, single detectors, such as TianQin and TianQin I+II; multiple detector networks, such as TianQin+LISA and TianQin I+II+LISA; and multi-band GW detector network, such as TianQin+ET and TianQin I+II+ET. The redshift information is obtained statistically from the photometric survey galaxy catalog by matching the sky localization and possible redshift range of the SBBH sources with the position and redshift of galaxies (we adopt the GWENS catalog in this work). Two methods are used to assign the weight of galaxies, including the fiducial method, in which each galaxy within the error box has a uniform weight, and the weighted method, in which the weight of a galaxy is proportional to the total stellar mass of the galaxy derived from the multi-band luminosity through the Le Phare method.

In comparison to single detector detection, both multi-detector networks and multi-band GW observations can significantly improve detection rates and spatial localization. As compared with the fiducial method, the weighted method can significantly improve the constraint precision of the Hubble constant. Using the fiducial method and the weighted method, in the TianQin scenario, the constraint precision of

H_0 is expected to be approximately 36.8% and approximately 30.9%, respectively; in the TianQin I+II detection scenario, the precision of H_0 is expected to be approximately 26.3% and approximately 14.4%, respectively. Using the weighted method, the constraint precision of H_0 in the TianQin+LISA and TianQin I+II+LISA detection scenarios is expected to be approximately 11.6% and approximately 4.1%, respectively. In the multi-band GW detection scenarios, the precision of the H_0 constrain by using the weighted method can approach around 1.5% and 1.1% under TianQin+ET configuration and TianQin I+II+ET configuration, respectively. It should be emphasized that both the weighted method and the multi-band GW detection significantly improve the constraint of H_0 .

Apart from H_0 , the space-borne GW detector can hardly constrain any other cosmological parameter, such as Ω_M , through the detections of SBBH inspiral GW signals. However, other cosmological parameters can be constrained by other types of GW sources, such as MBHB mergers [87, 88, 92]. MBHB sources generally have a very high SNRs, and their event horizons can extend to high redshifts ($z \gg 1$). As a result, combining SBBH and MBHB GW observations enables a more thorough analysis of GW cosmology study.

Additionally, we study the extent to which spectroscopic redshift information improves the constraining power of the Hubble constant, which increases not just the precision of the Hubble constant but also the accuracy of the constraint. Finally, we evaluated the reliability of our Bayesian analysis framework and galaxy weighting method using the *P-P* plot method by performing a consistency test.

Certain concerns remain unresolved for future studies, such as incorporating a complete frequency response [141] or the time-delay interferometry response [213]. MCMC can also be used in place of the FIM method to obtain more realistic GW parameter estimations [214]. The calibration uncertainty of the laser interferometer on the ground-based GW detector might result in systematic errors in the luminosity distance measurement [215-217], such as for ET. We reserve such issues for future investigations.

This work was supported by the Guangdong Major Project of Basic and Applied Basic Research (Grant No. 2019B030302001), the National Natural Science Foundation of China (Grant Nos. 12173104, 11805286, and 11690022), and the National Key Research and Development Program of China (Grant No. 2020YFC2201400). We acknowledge the use of the Kunlun cluster, a supercomputer owned by the School of Physics and Astronomy, Sun Yat-Sen University, and of the Tianhe-2, a supercomputer owned by the National Supercomputing Center in GuangZhou. The authors acknowledge the uses of the calculating utilities of emcee, numpy, scipy, and LALSuite, and the plotting utilities of matplotlib, and corner. The authors also thank Xiao-Dong Li, Martin Hendry, and Han Wang for helpful discussions.

- 2 P. A. R. Ade, et al. (Planck Collaboration), *Astron. Astrophys.* **594**, A13 (2016), arXiv: [1502.01589](#).
- 3 N. Aghanim, et al. (Planck Collaboration), *Astron. Astrophys.* **641**, A6 (2020), arXiv: [1807.06209](#).
- 4 W. L. Freedman, *Nat. Astron.* **1**, 0121 (2017), arXiv: [1706.02739](#).
- 5 W. L. Freedman, B. F. Madore, D. Hatt, T. J. Hoyt, I. S. Jang, R. L. Beaton, C. R. Burns, M. G. Lee, A. J. Monson, J. R. Neeley, M. M. Phillips, J. A. Rich, and M. Seibert, *Astrophys. J.* **882**, 34 (2019), arXiv: [1907.05922](#).
- 6 W. L. Freedman, *Astrophys. J.* **919**, 16 (2021), arXiv: [2106.15656](#).
- 7 A. G. Riess, S. Casertano, W. Yuan, L. M. Macri, and D. Scolnic, *Astrophys. J.* **876**, 85 (2019), arXiv: [1903.07603](#).
- 8 A. G. Riess, *Nat. Rev. Phys.* **2**, 10 (2020), arXiv: [2001.03624](#).
- 9 A. G. Riess, S. Casertano, W. Yuan, J. B. Bowers, L. Macri, J. C. Zinn, and D. Scolnic, *Astrophys. J. Lett.* **908**, L6 (2021), arXiv: [2012.08534](#).
- 10 H. Y. Chen, M. Fishbach, and D. E. Holz, *Nature* **562**, 545 (2018), arXiv: [1712.06531](#).
- 11 S. M. Feeney, H. V. Peiris, A. R. Williamson, S. M. Nissanke, D. J. Mortlock, J. Alsing, and D. Scolnic, *Phys. Rev. Lett.* **122**, 061105 (2019), arXiv: [1802.03404](#).
- 12 S. Borhanian, A. Dhani, A. Gupta, K. G. Arun, and B. S. Sathyaprakash, *Astrophys. J.* **905**, L28 (2020).
- 13 L. Bian, R.-G. Cai, S. Cao, Z. Cao, H. Gao, Z.-K. Guo, K. Lee, D. Li, J. Liu, Y. Lu, S. Pi, J.-M. Wang, S.-J. Wang, Y. Wang, T. Yang, X.-Y. Yang, S. Yu, and X. Zhang, *Sci. China-Phys. Mech. Astron.* **64**, 120401 (2021), arXiv: [2106.10235](#).
- 14 B. P. Abbott, et al. (LIGO Scientific Collaboration and Virgo Collaboration), *Phys. Rev. Lett.* **116**, 061102 (2016), arXiv: [1602.03837](#).
- 15 B. P. Abbott, et al. (LIGO Scientific Collaboration and Virgo Collaboration), *Phys. Rev. Lett.* **116**, 241103 (2016), arXiv: [1606.04855](#).
- 16 B. P. Abbott, et al. (LIGO Scientific Collaboration and Virgo Collaboration), *Phys. Rev. Lett.* **118**, 221101 (2017), arXiv: [1706.01812](#).
- 17 B. P. Abbott, et al. (LIGO Scientific Collaboration and Virgo Collaboration), *Astrophys. J.* **851**, L35 (2017), arXiv: [1711.05578](#).
- 18 B. P. Abbott, et al. (LIGO Scientific Collaboration and Virgo Collaboration), *Phys. Rev. Lett.* **119**, 141101 (2017), arXiv: [1709.09660](#).
- 19 B. P. Abbott, et al. (LIGO Scientific Collaboration and Virgo Collaboration), *Phys. Rev. Lett.* **119**, 161101 (2017), arXiv: [1710.05832](#).
- 20 B. P. Abbott, et al. (LIGO Scientific Collaboration and Virgo Collaboration), *Phys. Rev. X* **9**, 031040 (2019), arXiv: [1811.12907](#).
- 21 R. Abbott, et al. (LIGO Scientific Collaboration and Virgo Collaboration), *Phys. Rev. D* **102**, 043015 (2020), arXiv: [2004.08342](#).
- 22 B. P. Abbott, et al. (LIGO Scientific Collaboration and Virgo Collaboration), *Astrophys. J. Lett.* **892**, L3 (2020), arXiv: [2001.01761](#).
- 23 R. Abbott, et al. (LIGO Scientific Collaboration and Virgo Collaboration), *Phys. Rev. Lett.* **125**, 101102 (2020), arXiv: [2009.01075](#).
- 24 R. Abbott, et al. (LIGO Scientific Collaboration and Virgo Collaboration), *Astrophys. J. Lett.* **896**, L44 (2020), arXiv: [2006.12611](#).
- 25 R. Abbott, et al. (LIGO Scientific Collaboration and Virgo Collaboration), *Phys. Rev. X* **11**, 021053 (2021), arXiv: [2010.14527](#).
- 26 R. Abbott, et al. (LIGO Scientific Collaboration and Virgo Collaboration), arXiv: [2108.01045](#).
- 27 R. Abbott, et al. (LIGO Scientific Collaboration and Virgo Collaboration), *Astrophys. J. Lett.* **915**, L5 (2021), arXiv: [2106.15163](#).
- 28 T. Akutsu, et al. (KAGRA), *Nat. Astron.* **3**, 35 (2019).
- 29 C. S. Unnikrishnan, *Int. J. Mod. Phys. D* **22**, 1341010 (2013), arXiv: [1510.06059](#).
- 30 S. Nissanke, D. E. Holz, N. Dalal, S. A. Hughes, J. L. Sievers, and C. M. Hirata, arXiv: [1307.2638](#).
- 31 S. Vitale, and H. Y. Chen, *Phys. Rev. Lett.* **121**, 021303 (2018), arXiv: [1804.07337](#).
- 32 D. J. Mortlock, S. M. Feeney, H. V. Peiris, A. R. Williamson, and S. M. Nissanke, *Phys. Rev. D* **100**, 103523 (2019), arXiv: [1811.11723](#).
- 33 B. P. Abbott, et al. (LIGO Scientific Collaboration and Virgo Collaboration), *Astrophys. J.* **848**, L13 (2017), arXiv: [1710.05834](#).
- 34 M. Soares-Santos, D. E. Holz, J. Annis, R. Chornock, K. Herner, E. Berger, D. Brout, H. Y. Chen, R. Kessler, M. Sako, S. Allam, D. L. Tucker, R. E. Butler, A. Palmese, Z. Doctor, H. T. Diehl, J. Friedman, B. Yanny, H. Lin, D. Scolnic, P. Cowperthwaite, E. Neilson, J. Marriner, N. Kuropatkin, W. G. Hartley, F. Paz-Chinchón, K. D. Alexander, E. Balbinot, P. Blanchard, D. A. Brown, J. L. Carlin, C. Conselice, E. R. Cook, A. Drlica-Wagner, M. R. Drout, F. Durret, T. Eftekhari, B. Farr, D. A. Finley, R. J. Foley, W. Fong, C. L. Fryer, J. García-Bellido, M. S. S. Gill, R. A. Gruendl, C. Hanna, D. Kasen, T. S. Li, P. A. A. Lopes, A. C. C. Lourenço, R. Margutti, J. L. Marshall, T. Matheson, G. E. Medina, B. D. Metzger, R. R. Muñoz, J. Muir, M. Nicholl, E. Quataert, A. Rest, M. Sauseda, D. J. Schlegel, L. F. Secco, F. Sobreira, A. Stebbins, V. A. Villar, K. Vivas, A. R. Walker, W. Wester, P. K. G. Williams, A. Zenteno, Y. Zhang, T. M. C. Abbott, F. B. Abdalla, M. Banerji, K. Bechtol, A. Benoit-Lévy, E. Bertin, D. Brooks, E. Buckley-Geer, D. L. Burke, A. C. Rosell, M. C. Kind, J. Carretero, F. J. Castander, M. Crocce, C. E. Cunha, C. B. D'Andrea, L. N. Costa, C. Davis, S. Desai, J. P. Dietrich, P. Doel, T. F. Eifler, E. Fernandez, B. Flaugher, P. Fosalba, E. Gaztanaga, D. W. Gerdes, T. Giannantonio, D. A. Goldstein, D. Gruen, J. Gschwend, G. Gutierrez, K. Honscheid, B. Jain, D. J. James, T. Jeltema, M. W. G. Johnson, M. D. Johnson, S. Kent, E. Krause, R. Kron, K. Kuehn, S. Kuhlmann, O. Lahav, M. Lima, M. A. G. Maia, M. March, R. G. McMahon, F. Menanteau, R. Miquel, J. J. Mohr, R. C. Nichol, B. Nord, R. L. C. Ogando, D. Petracick, A. A. Plazas, A. K. Romer, A. Roodman, E. S. Rykoff, E. Sanchez, V. Scarpine, M. Schubnell, I. Sevilla-Noarbe, M. Smith, R. C. Smith, E. Suchyta, M. E. C. Swanson, G. Tarle, D. Thomas, R. C. Thomas, M. A. Troxel, V. Vikram, R. H. Wechsler, and J. Weller, *Astrophys. J.* **848**, L16 (2017), arXiv: [1710.05459](#).
- 35 B. P. Abbott, et al. (SKA South Africa/MeerKAT), *Astrophys. J.* **848**, L12 (2017), arXiv: [1710.05833](#).
- 36 B. P. Abbott, et al. (LIGO Scientific Collaboration and Virgo Collaboration), *Astrophys. J.* **909**, 218 (2021), arXiv: [1908.06060](#).
- 37 B. P. Abbott, R. Abbott, T. D. Abbott, F. Acernese, K. Ackley, C. Adams, T. Adams, P. Addesso, R. X. Adhikari, and V. B. Adya, *Nature* **551**, 85 (2017), arXiv: [1710.05835](#).
- 38 M. Fishbach, R. Gray, I. M. Hernandez, H. Qi, A. Sur, F. Acernese, L. Aiello, A. Allocca, M. A. Aloy, A. Amato, S. Antier, M. Aréne, N. Arnaud, S. Ascenzi, P. Astone, F. Aubin, S. Babak, P. Bacon, F. Badaracco, M. K. M. Bader, F. Baldaccini, G. Ballardin, F. Barone, M. Barsuglia, D. Barta, A. Basti, M. Bawaj, M. Bazzan, M. Bejger, I. Belahcene, S. Bernuzzi, D. Bersanetti, A. Bertolini, M. Bitossi, M. A. Bizouard, C. D. Blair, S. Bloemen, M. Boer, G. Bogaert, F. Bondu, R. Bonnand, B. A. Boom, V. Boschi, Y. Bouffanais, A. Bozzi, C. Bradascia, P. R. Brady, M. Branchesi, T. Briant, F. Brighenti, A. Brillet, V. Brisson, T. Bulik, H. J. Bulten, D. Buskulic, C. Buy, G. Cagnoli, E. Calloni, M. Canepa, E. Capocasa, F. Carbognani, G. Carullo, J. C. Diaz, C. Casentini, S. Caudill, F. Cavalier, R. Cavalieri, G. Celli, P. Cerdá-Durán, G. Cerretani, E. Cesaroni, O. Chaibi, E. Chassande-Mottin, K. Chatzilios, H. Y. Chen, A. Chincarini, A. Chiummo, N. Christensen, S. Chua, G. Ciani, R. Ciolfi, F. Cipriano, A. Cirone, F. Cleva, E. Coccia, P. F. Cohadon, D. Cohen, L. Conti, I. Cordero-Carrión, S. Cortese, M. W. Coughlin, J. P. Coulon, M. Croquette, E. Cuoco, G. Dálya, S. D'Antonio, L. E. H. Datrier, V. Dattilo, M. Davier, J. Degallaix, M. D. Laurentis, S. Deléglise, W. D. Pozzo, M. Denys, R. D. Pietri, R. D. Rosa, C. D. Rossi, R. DeSalvo, T. Dietrich, L. D. Fiore, M. D. Giovanni, T. D. Girolamo, A. D. Lieto, S. D. Pace, I. D. Palma, F. D. Renzo, Z. Doctor, M. Drago, J. G. Ducoin, M. Eisenmann, R. C. Essick, D. Estevez, V. Fafone, S. Farinon, W. M. Farr, F. Feng, I. Ferrante, F. Ferrini, F. Fidecaro, I. Fiori, D. Fiorucci, R. Flaminio, J. A. Font, J. D. Fournier, S. Frasca, F. Frasconi, V. Frey, J. R. Gair, L. Gammaiton, F. Garufi, G. Gemme, E. Genin, A. Gennai, D. George, V. Germain, A. Ghosh, B. Giacomazzo, A. Giazotto, G. Giordano, J. M. G. Castro, M. Gosselin, R. Gouaty, A. Grado, M. Granata, G. Greco, P. Groot, P. Gruning, G. M. Guidi, Y. Guo, O. Halim, J. Harms, C. J. Haster, A. Heidmann, H. Heitmann, P. Hello, G. Hemming, M. Hendry, T. Hinderer, D. Hoak, D. Hofman, D. E. Holz, A. Hreibi, D. Huet, B. Idzkowski, A. Iess,

- G. Intini, J. M. Isaac, T. Jacqmin, P. Jaradowski, R. J. G. Jonker, S. Katsanevas, E. Katsavounidis, F. Kéfélian, I. Khan, G. Koekoek, S. Koley, I. Kowalska, A. Królak, A. Kutynia, J. Lange, A. Lartaux-Vollard, C. Lazzaro, P. Leaci, N. Letendre, T. G. F. Li, F. Linde, A. Longo, M. Lorenzini, V. Loriette, G. Losurdo, D. Lumaca, R. Macas, A. Macquet, E. Majorana, I. Maksimovic, N. Man, M. Mantovani, F. Marchesoni, C. Markakis, A. Marquina, F. Martelli, E. Massera, A. Masserot, S. Mastrogiovanni, J. Meidam, L. Mereni, M. Merzougui, C. Messenger, R. Metzdorff, C. Michel, L. Milano, A. Miller, O. Minazzoli, Y. Minenkov, M. Montani, S. Morisaki, B. Mours, A. Nagar, I. Nardecchia, L. Naticchioni, G. Nelemans, D. Nichols, F. Nocera, M. Obergaulinger, G. Pagano, C. Palomba, F. Pannarale, F. Paoletti, A. Paoli, A. Pasqualetti, R. Passaquieti, D. Passuello, M. Patil, B. Patricelli, R. Pedurand, A. Perreca, O. J. Piccinni, M. Pichot, F. Piergiovanni, G. Pillant, L. Pinard, R. Poggiani, P. Popolizio, G. A. Prodi, M. Punturo, P. Puppo, N. Radulescu, P. Raffai, P. Rapagnani, V. Raymond, M. Razzano, T. Regimbau, L. Rei, F. Ricci, A. Rocchi, L. Rolland, M. Romanelli, R. Romano, D. Rosińska, P. Ruggi, L. Salconi, A. Samajdar, N. Sanchis-Gual, B. Sassolas, B. F. Schutz, D. Sentenac, V. Sequino, M. Sieniawska, N. Singh, A. Singhal, F. Sorrentino, C. Stachie, D. A. Steer, G. Stratta, B. L. Swinkels, M. Tacca, N. Tamanini, S. Tiwari, M. Tonelli, A. Torres-Forné, F. Travassos, M. C. Tringali, A. Trovato, L. Trozzo, K. W. Tsang, N. Bakel, M. Beuzekom, J. F. J. Brand, C. V. D. Broeck, L. Schaaf, J. V. Heijningen, M. Vardaro, M. Vasúth, G. Vedovato, J. Veitch, D. Verkindt, F. Vetrano, A. Viceré, J. Y. Vinet, H. Vocca, R. Walet, G. Wang, Y. F. Wang, M. Was, A. R. Williamson, M. Yvert, A. Zadrożny, T. Zelenova, J. P. Zendri, and A. B. Zimmerman, *Astrophys. J.* **871**, L13 (2019), arXiv: [1807.05667](#).
- 39 C. Guidorzi, R. Margutti, D. Brout, D. Scolnic, W. Fong, K. D. Alexander, P. S. Cowperthwaite, J. Annis, E. Berger, P. K. Blanchard, R. Chornock, D. L. Coppejans, T. Eftekhar, J. A. Frieman, D. Huterer, M. Nicholl, M. Soares-Santos, G. Terreran, V. A. Villar, and P. K. G. Williams, *Astrophys. J.* **851**, L36 (2017), arXiv: [1710.06426](#).
- 40 K. Hotokezaka, E. Nakar, O. Gottlieb, S. Nissanke, K. Masuda, G. Hallinan, K. P. Mooley, and A. T. Deller, *Nat. Astron.* **3**, 940 (2019), arXiv: [1806.10596](#).
- 41 B. McKernan, K. E. S. Ford, I. Bartos, M. J. Graham, W. Lyra, S. Marka, Z. Marka, N. P. Ross, D. Stern, and Y. Yang, *Astrophys. J.* **884**, L50 (2019), arXiv: [1907.03746](#).
- 42 M. J. Graham, K. E. S. Ford, B. McKernan, N. P. Ross, D. Stern, K. Burdge, M. Coughlin, S. G. Djorgovski, A. J. Drake, D. Duev, M. Kasliwal, A. A. Mahabal, S. van Velzen, J. Belecki, E. C. Bellm, R. Burruas, S. B. Cenko, V. Cunningham, G. Helou, S. R. Kulkarni, F. J. Masci, T. Prince, D. Reiley, H. Rodriguez, B. Rusholme, R. M. Smith, and M. T. Soumagnac, *Phys. Rev. Lett.* **124**, 251102 (2020), arXiv: [2006.14122](#).
- 43 M. Soares-Santos, et al. (The LIGO Scientific Collaboration and the Virgo Collaboration), *Astrophys. J.* **876**, L7 (2019), arXiv: [1901.01540](#).
- 44 A. Palmese, et al. (DES Collaboration), *Astrophys. J.* **900**, L33 (2020), arXiv: [2006.14961](#).
- 45 S. S. Vasylyev, and A. V. Filippenko, *Astrophys. J.* **902**, 149 (2020), arXiv: [2007.11148](#).
- 46 W. Del Pozzo, *Phys. Rev. D* **86**, 043011 (2012), arXiv: [1108.1317](#).
- 47 S. R. Taylor, J. R. Gair, and I. Mandel, *Phys. Rev. D* **85**, 023535 (2012), arXiv: [1108.5161](#).
- 48 R. Nair, S. Bose, and T. D. Saini, *Phys. Rev. D* **98**, 023502 (2018), arXiv: [1804.06085](#).
- 49 W. M. Farr, M. Fishbach, J. Ye, and D. E. Holz, *Astrophys. J.* **883**, L42 (2019), arXiv: [1908.09084](#).
- 50 R. Gray, I. M. Hernandez, H. Qi, A. Sur, P. R. Brady, H. Y. Chen, W. M. Farr, M. Fishbach, J. R. Gair, A. Ghosh, D. E. Holz, S. Mastrogiovanni, C. Messenger, D. A. Steer, and J. Veitch, *Phys. Rev. D* **101**, 122001 (2020), arXiv: [1908.06050](#).
- 51 S. Bera, D. Rana, S. More, and S. Bose, *Astrophys. J.* **902**, 79 (2020), arXiv: [2007.04271](#).
- 52 A. Finke, S. Foffa, F. Iacobelli, M. Maggiore, and M. Mancarella, *J. Cosmol. Astropart. Phys.* **2021**, 26 (2021), arXiv: [2101.12660](#).
- 53 R. Gray, C. Messenger, and J. Veitch, arXiv: [2111.04629](#).
- 54 R. Abbott, et al. (LIGO Scientific, VIRGO, KAGRA), arXiv: [2111.03604](#).
- 55 M. Punturo, M. Abernathy, F. Acernese, B. Allen, N. Andersson, K. Arun, F. Barone, B. Barr, M. Barsuglia, M. Beker, N. Beveridge, S. Birindelli, S. Bose, L. Bosi, S. Braccini, C. Bradaschia, T. Bulik, E. Calloni, G. Celli, E. C. Mottin, S. Chelkowski, A. Chincarini, J. Clark, E. Coccia, C. Colacino, J. Colas, A. Cumming, L. Cunningham, E. Cuoco, S. Danilishin, K. Danzmann, G. De Luca, R. De Salvo, T. Dent, R. De Rosa, L. Di Fiore, A. Di Virgilio, M. Doets, V. Fafone, P. Falferi, R. Flaminio, J. Franc, F. Frasconi, A. Freise, P. Fulda, J. Gair, G. Gemme, A. Gennai, A. Giazotto, K. Glampedakis, M. Granata, H. Grote, G. Guidi, G. Hammond, M. Hannam, J. Harms, D. Heinert, M. Hendry, I. Heng, E. Hennes, S. Hild, J. Hough, S. Husa, S. Huttner, G. Jones, F. Khalili, K. Kokeyama, K. Kokkotas, B. Krishnan, M. Lorenzini, H. Lück, E. Majorana, I. Mandel, V. Mandic, I. Martin, C. Michel, Y. Minenkov, N. Morgado, S. Mosca, B. Mours, H. Müller-Ebhardt, P. Murray, R. Nawrodt, J. Nelson, R. Oshaughnessy, C. D. Ott, C. Palomba, A. Paoli, G. Parguez, A. Pasqualetti, R. Passaquieti, D. Passuello, L. Pinard, R. Poggiani, P. Popolizio, M. Prato, P. Puppo, D. Rabeling, P. Rapagnani, J. Read, T. Regimbau, H. Rehbein, S. Reid, L. Rezzolla, F. Ricci, F. Richard, A. Rocchi, S. Rowan, A. Rüdiger, B. Sassolas, B. Sathyaprakash, R. Schnabel, C. Schwarz, P. Seidel, A. Sintes, K. Somiya, F. Speirits, K. Strain, S. Strigin, P. Sutton, S. Tarabrin, A. Thüring, J. van den Brand, C. van Leewen, M. van Veggel, C. van den Broeck, A. Vecchio, J. Veitch, F. Vetrano, A. Vicere, S. Vyatchanin, B. Willke, G. Woan, P. Wolfango, and K. Yamamoto, *Class. Quantum Grav.* **27**, 194002 (2010).
- 56 B. Sathyaprakash, M. Abernathy, F. Acernese, P. Ajith, B. Allen, P. Amaro-Seoane, N. Andersson, S. Aoudia, K. Arun, P. Astone, B. Krishnan, L. Barack, F. Barone, B. Barr, M. Barsuglia, M. Bassan, R. Bassiri, M. Beker, N. Beveridge, M. Bizouard, C. Bond, S. Bose, L. Bosi, S. Braccini, C. Bradaschia, M. Britzger, F. Brueckner, T. Bulik, H. J. Bulten, O. Burmeister, E. Calloni, P. Campsie, L. Carbone, G. Celli, E. Chalkley, E. Chassande-Mottin, S. Chelkowski, A. Chincarini, A. D. Cintio, J. Clark, E. Coccia, C. N. Colacino, J. Colas, A. Colla, A. Corsi, A. Cumming, L. Cunningham, E. Cuoco, S. Danilishin, K. Danzmann, E. Daw, R. De Salvo, W. D. Pozzo, T. Dent, R. De Rosa, L. D. Fiore, M. D. P. Emilio, A. D. Virgilio, A. Dietz, M. Doets, J. Dueck, M. Edwards, V. Fafone, S. Fairhurst, P. Falferi, M. Favata, V. Ferrari, F. Ferrini, F. Fidecaro, R. Flaminio, J. Franc, F. Frasconi, A. Freise, D. Friedrich, P. Fulda, J. Gair, M. Galimberti, G. Gemme, E. Genin, A. Gennai, A. Giazotto, K. Glampedakis, S. Gossan, R. Gouaty, C. Graef, W. Graham, M. Granata, H. Grote, G. Guidi, J. Hallam, G. Hammond, M. Hannam, J. Harms, K. Haughian, I. Hawke, D. Heinert, M. Hendry, I. Heng, E. Hennes, S. Hild, J. Hough, D. Huet, S. Husa, S. Huttner, B. Iyer, D. I. Jones, G. Jones, I. Kamaretsos, C. K. Mishra, F. Kawazoe, F. Khalili, B. Kley, K. Kokeyama, K. Kokkotas, S. Kroker, R. Kumar, K. Kuroda, B. Lagrange, N. Lastzka, T. G. F. Li, M. Lorenzini, G. Losurdo, H. Lück, E. Majorana, V. Malvezzi, I. Mandel, V. Mandic, S. Marka, F. Marin, F. Marion, J. Marque, I. Martin, D. M. Leod, D. McKechnan, M. Mehmet, C. Michel, Y. Minenkov, N. Morgado, A. Morgia, S. Mosca, L. Moscatelli, B. Mours, H. Müller-Ebhardt, P. Murray, L. Naticchioni, R. Nawrodt, J. Nelson, R. O. Shaughnessy, C. D. Ott, C. Palomba, A. Paoli, G. Parguez, A. Pasqualetti, R. Passaquieti, D. Passuello, M. Perciballi, F. Piergiovanni, L. Pinard, M. Pitkin, W. Plastino, M. Plissi, R. Poggiani, P. Popolizio, E. Porter, M. Prato, G. Prodi, M. Punturo, P. Puppo, D. Rabeling, I. Racz, P. Rapagnani, V. Re, J. Read, T. Regimbau, H. Rehbein, S. Reid, F. Ricci, F. Richard, C. Robinson, A. Rocchi, R. Romano, S. Rowan, A. Rüdiger, A. Sambowski, L. Santamaría, B. Sassolas, R. Schilling, P. Schmidt, R. Schnabel, B. Schutz, C. Schwarz, J. Scott, P. Seidel, A. M. Sintes, K. Somiya, C. F. Sopuerta, B. Sorazu, F. Speirits, L. Storch, K. Strain,

- S. Stringin, P. Sutton, S. Tarabrin, B. Taylor, A. Thürin, K. Tokmakov, M. Tonelli, H. Tournefier, R. Vaccarone, H. Vahlbruch, J. F. J. van den Brand, C. Van Den Broeck, S. van der Putten, M. van Veggel, A. Vecchio, J. Veitch, F. Vetrano, A. Vicere, S. Vyatchanin, P. Weßels, B. Willke, W. Winkler, G. Woan, A. Woodcraft, and K. Yamamoto, *Class. Quantum Grav.* **29**, 124013 (2012), arXiv: [1206.0331](#).
- 57 S. Dwyer, D. Sigg, S. W. Ballmer, L. Barsotti, N. Mavalvala, and M. Evans, *Phys. Rev. D* **91**, 082001 (2015), arXiv: [1410.0612](#).
- 58 B. P. Abbott, et al. (LIGO Scientific Collaboration and Virgo Collaboration), *Class. Quantum Grav.* **34**, 044001 (2017), arXiv: [1607.08697](#).
- 59 W. Zhao, C. van den Broeck, D. Baskaran, and T. G. F. Li, *Phys. Rev. D* **83**, 023005 (2011), arXiv: [1009.0206](#).
- 60 W. Zhao, and L. Wen, *Phys. Rev. D* **97**, 064031 (2018), arXiv: [1710.05325](#).
- 61 S. R. Taylor, and J. R. Gair, *Phys. Rev. D* **86**, 023502 (2012), arXiv: [1204.6739](#).
- 62 M. Siekel, C. Clarkson, and M. Smith, *J. Cosmol. Astropart. Phys.* **2012**, 036 (2012), arXiv: [1204.2832](#).
- 63 C. Messenger, and J. Read, *Phys. Rev. Lett.* **108**, 091101 (2012), arXiv: [1107.5725](#).
- 64 C. Messenger, K. Takami, S. Gossan, L. Rezzolla, and B. S. Sathyaprakash, *Phys. Rev. X* **4**, 041004 (2014), arXiv: [1312.1862](#).
- 65 W. Del Pozzo, T. G. F. Li, and C. Messenger, *Phys. Rev. D* **95**, 043502 (2017), arXiv: [1506.06590](#).
- 66 R. G. Cai, and T. Yang, *Phys. Rev. D* **95**, 044024 (2017), arXiv: [1608.08008](#).
- 67 M. Du, W. Yang, L. Xu, S. Pan, and D. F. Mota, *Phys. Rev. D* **100**, 043535 (2019), arXiv: [1812.01440](#).
- 68 X. N. Zhang, L. F. Wang, J. F. Zhang, and X. Zhang, *Phys. Rev. D* **99**, 063510 (2019), arXiv: [1804.08379](#).
- 69 J. M. S. de Souza, and R. Sturani, *Phys. Dark Univ.* **32**, 100830 (2021), arXiv: [1905.03848](#).
- 70 J. F. Zhang, M. Zhang, S. J. Jin, J. Z. Qi, and X. Zhang, *J. Cosmol. Astropart. Phys.* **2019(9)**, 068 (2019), arXiv: [1907.03238](#).
- 71 J. Yu, Y. Wang, W. Zhao, and Y. Lu, *Mon. Not. R. Astron. Soc.* **498**, 1786 (2020), arXiv: [2003.06586](#).
- 72 Z. Q. You, X. J. Zhu, G. Ashton, E. Thrane, and Z. H. Zhu, *Astrophys. J.* **908**, 215 (2021), arXiv: [2004.00036](#).
- 73 A. Bonilla, S. Kumar, R. C. Nunes, and S. Pan, arXiv: [2102.06149](#).
- 74 J. Luo, L. S. Chen, H. Z. Duan, Y. G. Gong, S. Hu, J. Ji, Q. Liu, J. Mei, V. Milyukov, M. Sazhin, C. G. Shao, V. T. Toth, H. B. Tu, Y. Wang, Y. Wang, H. C. Yeh, M. S. Zhan, Y. Zhang, V. Zharov, and Z. B. Zhou, *Class. Quantum Grav.* **33**, 035010 (2016), arXiv: [1512.02076](#).
- 75 P. Amaro-Seoane, et al. (LISA Collaboration), arXiv: [1702.00786](#).
- 76 A. Klein, E. Barausse, A. Sesana, A. Petiteau, E. Berti, S. Babak, J. Gair, S. Aoudia, I. Hinder, F. Ohme, and B. Wardell, *Phys. Rev. D* **93**, 024003 (2016), arXiv: [1511.05581](#).
- 77 E. Barausse, I. Dvorkin, M. Tremmel, M. Volonteri, and M. Bonetti, *Astrophys. J.* **904**, 16 (2020), arXiv: [2006.03065](#).
- 78 H. T. Wang, Z. Jiang, A. Sesana, E. Barausse, S. J. Huang, Y. F. Wang, W. F. Feng, Y. Wang, Y. M. Hu, J. Mei, and J. Luo, *Phys. Rev. D* **100**, 043003 (2019), arXiv: [1902.04423](#).
- 79 S. Babak, J. Gair, A. Sesana, E. Barausse, C. F. Sopuerta, C. P. L. Berry, E. Berti, P. Amaro-Seoane, A. Petiteau, and A. Klein, *Phys. Rev. D* **95**, 103012 (2017), arXiv: [1703.09722](#).
- 80 J. R. Gair, S. Babak, A. Sesana, P. Amaro-Seoane, E. Barausse, C. P. L. Berry, E. Berti, and C. Sopuerta, *J. Phys.-Conf. Ser.* **840**, 012021 (2017), arXiv: [1704.00009](#).
- 81 H. M. Fan, Y. M. Hu, E. Barausse, A. Sesana, J. Zhang, X. Zhang, T. G. Zi, and J. Mei, *Phys. Rev. D* **102**, 063016 (2020), arXiv: [2005.08212](#).
- 82 K. Kyutoku, and N. Seto, *Mon. Not. R. Astron. Soc.* **462**, 2177 (2016), arXiv: [1606.02298](#).
- 83 S. Liu, Y. M. Hu, J. Zhang, and J. Mei, *Phys. Rev. D* **101**, 103027 (2020), arXiv: [2004.14242](#).
- 84 S. Liu, L. G. Zhu, Y. M. Hu, J. Zhang, and M. J. Ji, *Phys. Rev. D* **105**, 023019 (2022).
- 85 D. E. Holz, and S. A. Hughes, *Astrophys. J.* **629**, 15 (2005), arXiv: [astro-ph/0504616](#).
- 86 S. Babak, J. R. Gair, A. Petiteau, and A. Sesana, *Class. Quantum Grav.* **28**, 114001 (2011), arXiv: [1011.2062](#).
- 87 A. Petiteau, S. Babak, and A. Sesana, *Astrophys. J.* **732**, 82 (2011), arXiv: [1102.0769](#).
- 88 N. Tamanini, C. Caprini, E. Barausse, A. Sesana, A. Klein, and A. Petiteau, *J. Cosmol. Astropart. Phys.* **2016(4)**, 002 (2016), arXiv: [1601.07112](#).
- 89 C. Caprini, and N. Tamanini, *J. Cosmol. Astropart. Phys.* **2016**, 6 (2016), arXiv: [1607.08755](#).
- 90 R. G. Cai, N. Tamanini, and T. Yang, *J. Cosmol. Astropart. Phys.* **2017**, 31 (2017), arXiv: [1703.07323](#).
- 91 L. F. Wang, Z. W. Zhao, J. F. Zhang, and X. Zhang, *J. Cosmol. Astropart. Phys.* **2020**, 012 (2020), arXiv: [1907.01838](#).
- 92 L.-G. Zhu, Y.-M. Hu, H.-T. Wang, J.-D. Zhang, X.-D. Li, M. Hendry, and J. Mei (2021), arXiv: [2104.11956](#).
- 93 R. Wang, W. H. Ruan, Q. Yang, Z. K. Guo, R. G. Cai, and B. Hu, *Natl. Sci. Rev.* **9**, nwab054 (2021).
- 94 L.-F. Wang, S.-J. Jin, J.-F. Zhang, and X. Zhang, *Sci. China-Phys. Mech. Astron.* **65**, 210411 (2022), arXiv: [2101.11882](#).
- 95 C. L. MacLeod, and C. J. Hogan, *Phys. Rev. D* **77**, 043512 (2008), arXiv: [0712.0618](#).
- 96 D. Laghi, N. Tamanini, W. Del Pozzo, A. Sesana, J. Gair, S. Babak, and D. Izquierdo-Villalba, *Mon. Not. R. Astron. Soc.* **508**, 4512 (2021), arXiv: [2102.01708](#).
- 97 K. Kyutoku, and N. Seto, *Phys. Rev. D* **95**, 083525 (2017), arXiv: [1609.07142](#).
- 98 W. Del Pozzo, A. Sesana, and A. Klein, *Mon. Not. R. Astron. Soc.* **475**, 3485 (2018), arXiv: [1703.01300](#).
- 99 A. Sesana, *Phys. Rev. Lett.* **116**, 231102 (2016), arXiv: [1602.06951](#).
- 100 A. Sesana, *J. Phys.-Conf. Ser.* **840**, 012018 (2017), arXiv: [1702.04356](#).
- 101 S. Vitale, *Phys. Rev. Lett.* **117**, 051102 (2016), arXiv: [1605.01037](#).
- 102 C. J. Moore, D. Gerosa, and A. Klein, *Mon. Not. R. Astron. Soc.-Lett.* **488**, L94 (2019), arXiv: [1905.11998](#).
- 103 B. Ewing, S. Sachdev, S. Borhanian, and B. S. Sathyaprakash, *Phys. Rev. D* **103**, 023025 (2021), arXiv: [2011.03036](#).
- 104 S. Grimm, and J. Harms, *Phys. Rev. D* **102**, 022007 (2020), arXiv: [2004.01434](#).
- 105 E. Barausse, N. Yunes, and K. Chamberlain, *Phys. Rev. Lett.* **116**, 241104 (2016), arXiv: [1603.04075](#).
- 106 K. W. K. Wong, E. D. Kovetz, C. Cutler, and E. Berti, *Phys. Rev. Lett.* **121**, 251102 (2018), arXiv: [1808.08247](#).
- 107 D. Gerosa, S. Ma, K. W. K. Wong, E. Berti, R. O'Shaughnessy, Y. Chen, and K. Belczynski, *Phys. Rev. D* **99**, 103004 (2019), arXiv: [1902.00021](#).
- 108 C. Cutler, E. Berti, K. Jani, E. D. Kovetz, L. Randall, S. Vitale, K. W. K. Wong, K. H. Bockelmann, S. L. Larson, T. Littenberg, S. T. McWilliams, G. Mueller, J. D. Schnittman, D. H. Shoemaker, and M. Vallisneri, arXiv: [1903.04069](#).
- 109 C. Liu, L. Shao, J. Zhao, and Y. Gao, *Mon. Not. R. Astron. Soc.* **496**, 182 (2020), arXiv: [2004.12096](#).
- 110 N. Muttoni, A. Mangiagli, A. Sesana, D. Laghi, W. Del Pozzo, and D. Izquierdo-Villalba, arXiv: [2109.13934](#).
- 111 J. Luo, Y. Z. Bai, L. Cai, B. Cao, W. M. Chen, Y. Chen, D. C. Cheng, Y. W. Ding, H. Z. Duan, X. Gou, C. Z. Gu, D. F. Gu, Z. Q. He, S. Hu, Y. Hu, X. Q. Huang, Q. Jiang, Y. Z. Jiang, H. G. Li, H. Y. Li, J. Li, M. Li, Z. Li, Z. X. Li, Y. R. Liang, F. J. Liao, Y. C. Liu, L. Liu, P. B. Liu, X. Liu, Y. Liu, X. F. Lu, Y. Luo, J. Mei, M. Ming, S. B. Qu, D. Y. Tan, M. Tang, L. C. Tu, C. R. Wang, F. Wang, G. F. Wang, J. Wang, L. Wang, X. Wang, R. Wei, S. C. Wu, C. Y. Xiao, M. Z. Xie, X. S. Xu, L. Yang, M. L. Yang, S. Q. Yang, H. C. Yeh, J. B. Yu, L. Zhang, M. H. Zhao, and Z. B. Zhou, *Class. Quantum Grav.* **37**, 185013 (2020), arXiv: [2008.09534](#).

- 112 J. Mei, Y. Z. Bai, J. Bao, E. Barausse, L. Cai, E. Canuto, B. Cao, W. M. Chen, Y. Chen, Y. W. Ding, H. Z. Duan, H. Fan, W. F. Feng, H. Fu, Q. Gao, T. Q. Gao, Y. Gong, X. Gou, C. Z. Gu, D. F. Gu, Z. Q. He, M. Hendry, W. Hong, X. C. Hu, Y. M. Hu, Y. Hu, S. J. Huang, X. Q. Huang, Q. Jiang, Y. Z. Jiang, Y. Jiang, Z. Jiang, H. M. Jin, V. Korol, H. Y. Li, M. Li, M. Li, P. Li, R. Li, Y. Li, Z. Li, Z. Li, Z. X. Li, Y. R. Liang, Z. C. Liang, F. J. Liao, Q. Liu, S. Liu, Y. C. Liu, L. Liu, P. B. Liu, X. Liu, Y. Liu, X. F. Lu, Y. Lu, Z. H. Lu, Y. Luo, Z. C. Luo, V. Milyukov, M. Ming, X. Pi, C. Qin, S. B. Qu, A. Sesana, C. Shao, C. Shi, W. Su, D. Y. Tan, Y. Tan, Z. Tan, L. C. Tu, B. Wang, C. R. Wang, F. Wang, G. F. Wang, H. Wang, J. Wang, L. Wang, P. Wang, X. Wang, Y. Wang, Y. F. Wang, R. Wei, S. C. Wu, C. Y. Xiao, X. S. Xu, C. Xue, F. C. Yang, L. Yang, M. L. Yang, S. Q. Yang, B. Ye, H. C. Yeh, S. Yu, D. Zhai, C. Zhang, H. Zhang, J. Zhang, J. Zhang, L. Zhang, X. Zhang, X. Zhang, H. Zhou, M. Y. Zhou, Z. B. Zhou, D. D. Zhu, T. G. Zi, and J. Luo, *Prog. Theor. Exp. Phys.* **2021**, 05A107 (2021), arXiv: [2008.10332](#).
- 113 M. Maggiore, C. V. D. Broeck, N. Bartolo, E. Belgacem, D. Bertacca, M. A. Bizouard, M. Branchesi, S. Clesse, S. Foffa, J. García-Bellido, S. Grimm, J. Harms, T. Hinderer, S. Matarrese, C. Palomba, M. Peloso, A. Ricciardone, and M. Sakellariadou, *J. Cosmol. Astropart. Phys.* **2020**, 050 (2020), arXiv: [1912.02622](#).
- 114 M. Colpi, and A. Sesana, *Gravitational Wave Sources in the Era of Multi-Band Gravitational Wave Astronomy* (World Scientific, Singapore, 2017), pp. 43–140.
- 115 W. Zhao, *Sci. Sin.-Phys. Mech. Astron.* **48**, 079805 (2018).
- 116 S. Nissanke, D. E. Holz, S. A. Hughes, N. Dalal, and J. L. Sievers, *Astrophys. J.* **725**, 496 (2010), arXiv: [0904.1017](#).
- 117 P. K. Blanchard, E. Berger, W. Fong, M. Nicholl, J. Leja, C. Conroy, K. D. Alexander, R. Margutti, P. K. G. Williams, Z. Doctor, R. Chornock, V. A. Villar, P. S. Cowperthwaite, J. Annis, D. Brout, D. A. Brown, H. Y. Chen, T. Eftekhari, J. A. Frieman, D. E. Holz, B. D. Metzger, A. Rest, M. Sako, and M. Soares-Santos, *Astrophys. J.* **848**, L22 (2017), arXiv: [1710.05458](#).
- 118 L. X. Li, and B. Paczyński, *Astrophys. J.* **507**, L59 (1998), arXiv: [astro-ph/9807272](#).
- 119 B. D. Metzger, G. Martínez-Pinedo, S. Darbha, E. Quataert, A. Arcones, D. Kasen, R. Thomas, P. Nugent, I. V. Panov, and N. T. Zinner, *Mon. Not. R. Astron. Soc.* **406**, 2650 (2010), arXiv: [1001.5029](#).
- 120 N. R. Tanvir, A. J. Levan, C. González-Fernández, O. Korobkin, I. Mandel, S. Rosswog, J. Hjorth, P. D’Avanzo, A. S. Fruchter, C. L. Fryer, T. Kangas, B. Milvang-Jensen, S. Rosetti, D. Steeghs, R. T. Wollaeger, Z. Cano, C. M. Copperwheat, S. Covino, V. D’Elia, A. de Ugarte Postigo, P. A. Evans, W. P. Even, S. Fairhurst, R. F. Jaimes, C. J. Fontes, Y. I. Fujii, J. P. U. Fynbo, B. P. Gompertz, J. Greiner, G. Hodosan, M. J. Irwin, P. Jakobsson, U. G. Jørgensen, D. A. Kann, J. D. Lyman, D. Malesani, R. G. McMahon, A. Melandri, P. T. O’Brien, J. P. Osborne, E. Palazzi, D. A. Perley, E. Pian, S. Piranomonte, M. Rabus, E. Rol, A. Rowlinson, S. Schulze, P. Sutton, C. C. Thöne, K. Ulaczyk, D. Watson, K. Wiersema, and R. A. M. J. Wijers, *Astrophys. J.* **848**, L27 (2017), arXiv: [1710.05455](#).
- 121 B. Kiziltan, A. Kottas, M. De Yoreo, and S. E. Thorsett, *Astrophys. J.* **778**, 66 (2013), arXiv: [1011.4291](#).
- 122 M. Oguri, *Phys. Rev. D* **93**, 083511 (2016), arXiv: [1603.02356](#).
- 123 P. Zhang, arXiv: [1811.07136](#).
- 124 S. Mukherjee, B. D. Wandelt, S. M. Nissanke, and A. Silvestri, *Phys. Rev. D* **103**, 043520 (2021), arXiv: [2007.02943](#).
- 125 C. C. Diaz, and S. Mukherjee, arXiv: [2107.12787](#).
- 126 X. Ding, M. Biesiada, X. Zheng, K. Liao, Z. Li, and Z. H. Zhu, *J. Cosmol. Astropart. Phys.* **2019**, 33 (2019), arXiv: [1801.05073](#).
- 127 H. Leandro, V. Marra, and R. Sturani, arXiv: [2109.07537](#).
- 128 N. Seto, S. Kawamura, and T. Nakamura, *Phys. Rev. Lett.* **87**, 221103 (2001), arXiv: [astro-ph/0108011](#).
- 129 A. Nishizawa, A. Taruya, and S. Saito, *Phys. Rev. D* **83**, 084045 (2011), arXiv: [1011.5000](#).
- 130 A. Nishizawa, K. Yagi, A. Taruya, and T. Tanaka, *Phys. Rev. D* **85**, 044047 (2012), arXiv: [1110.2865](#).
- 131 I. Mandel, W. M. Farr, and J. R. Gair, *Mon. Not. R. Astron. Soc.* **486**, 1086 (2019), arXiv: [1809.02063](#).
- 132 L. S. Finn, *Phys. Rev. D* **46**, 5236 (1992), arXiv: [gr-qc/9209010](#).
- 133 G. Dálya, G. Galgócz, L. Dobos, Z. Frei, I. S. Heng, R. Macas, C. Messenger, P. Raffai, and R. S. de Souza, *Mon. Not. R. Astron. Soc.* **479**, 2374 (2018), arXiv: [1804.05709](#).
- 134 K. S. Thorne, in *Three Hundred Years of Gravitation*, edited by S. W. Hawking, and W. Israel (Cambridge University Press, Cambridge, 1987), pp. 330–458.
- 135 A. Freise, S. Chelkowski, S. Hild, W. Del Pozzo, A. Perreca, and A. Vecchio, *Class. Quantum Grav.* **26**, 085012 (2009), arXiv: [0804.1036](#).
- 136 X. C. Hu, X. H. Li, Y. Wang, W. F. Feng, M. Y. Zhou, Y. M. Hu, S. C. Hu, J. W. Mei, and C. G. Shao, *Class. Quantum Grav.* **35**, 095008 (2018), arXiv: [1803.03368](#).
- 137 C. Cutler, *Phys. Rev. D* **57**, 7089 (1998), arXiv: [gr-qc/9703068](#).
- 138 N. J. Cornish, and L. J. Rubbo, *Phys. Rev. D* **67**, 022001 (2003). [Erratum: *Phys. Rev. D* **67**, 029905 (2003)].
- 139 P. Jaranowski, A. Królak, and B. F. Schutz, *Phys. Rev. D* **58**, 063001 (1998), arXiv: [gr-qc/9804014](#).
- 140 T. Robson, N. J. Cornish, and C. Liu, *Class. Quantum Grav.* **36**, 105011 (2019), arXiv: [1803.01944](#).
- 141 C. Zhang, Q. Gao, Y. Gong, B. Wang, A. J. Weinstein, and C. Zhang, *Phys. Rev. D* **101**, 124027 (2020), arXiv: [2003.01441](#).
- 142 C. Cutler, and É. E. Flanagan, *Phys. Rev. D* **49**, 2658 (1994), arXiv: [gr-qc/9402014](#).
- 143 S. Hild, M. Abernathy, F. Acernese, P. Amaro-Seoane, N. Andersson, K. Arun, F. Barone, B. Barr, M. Barsuglia, M. Beker, N. Beveridge, S. Birindelli, S. Bose, L. Bosi, S. Braccini, C. Bradaschia, T. Bulik, E. Calloni, G. Cella, E. C. Mottin, S. Chelkowski, A. Chincarini, J. Clark, E. Coccia, C. Colacino, J. Colas, A. Cumming, L. Cunningham, E. Cuoco, S. Danilishin, K. Danzmann, R. De Salvo, T. Dent, R. De Rosa, L. Di Fiore, A. Di Virgilio, M. Doets, V. Favone, P. Falferi, R. Flaminio, J. Franc, F. Frasconi, A. Freise, D. Friedrich, P. Fulda, J. Gair, G. Gemme, E. Genin, A. Gennai, A. Giacotto, K. Glampedakis, C. Gräf, M. Granata, H. Grote, G. Guidi, A. Gurkovsky, G. Hammond, M. Hannam, J. Harms, D. Heinert, M. Hendry, I. Heng, E. Hennes, J. Hough, S. Husa, S. Huttner, G. Jones, F. Khalili, K. Kokeyama, K. Kokkotas, B. Krishnan, T. G. F. Li, M. Lorenzini, H. Lück, E. Majorana, I. Mandel, V. Mandic, M. Mantovani, I. Martin, C. Michel, Y. Minenkov, N. Morgado, S. Mosca, B. Mours, H. MüllerCEhardt, P. Murray, R. Nawrodt, J. Nelson, R. Oshaughnessy, C. D. Ott, C. Palomba, A. Paoli, G. Parguez, A. Pasqualetti, R. Passaquieti, D. Passuello, L. Pinard, W. Plastino, R. Poggiani, P. Popolizio, M. Prato, M. Punturo, P. Puppo, D. Rabeling, P. Rapagnani, J. Read, T. Regimbau, H. Rehbein, S. Reid, F. Ricci, F. Richard, A. Rocchi, S. Rowan, A. Rüdiger, L. Santamaría, B. Sassolas, B. Sathyaprakash, R. Schnabel, C. Schwarz, P. Seidel, A. Sintes, K. Somiya, F. Speirits, K. Strain, S. Strigin, P. Sutton, S. Tarabrin, A. Thüring, J. van den Brand, M. van Veggel, C. van den Broeck, A. Vecchio, J. Veitch, F. Vetrano, A. Vicere, S. Vyatchanin, B. Willke, G. Woan, and K. Yamamoto, *Class. Quantum Grav.* **28**, 094013 (2011), arXiv: [1012.0908](#).
- 144 M. Vallisneri, *Phys. Rev. D* **77**, 042001 (2008), arXiv: [gr-qc/0703086](#).
- 145 E. F. Bell, D. H. McIntosh, N. Katz, and M. D. Weinberg, *Astrophys. J. Suppl. S* **149**, 289 (2003), arXiv: [astro-ph/0302543](#).
- 146 Y. T. Lin, J. J. Mohr, and S. A. Stanford, *Astrophys. J.* **610**, 745 (2004), arXiv: [astro-ph/0402308](#).
- 147 B. Abolfathi, D. S. Aguado, G. Aguilar, C. A. Prieto, A. Almeida, T. T. Ananna, F. Anders, S. F. Anderson, B. H. Andrews, B. Anguiano, A. Aragón-Salamanca, M. Argudo-Fernández, E. Armengaud, M. Ata, E. Aubourg, V. Avila-Reese, C. Badenes, S. Bailey, C. Balland, K. A. Barger, J. Barrera-Ballesteros, C. Bartosz, F. Bastien, D. Bates, F. Baumgarten, J. Bautista, R. Beaton, T. C. Beers, F. Belfiore, C. F. Bender, M. Bernardi, M. A. Bershadsky, F. Beutler, J. C. Bird, D. Bizyaev, G. A. Blanc, M. R. Blanton, M. Blomqvist, A. S. Bolton,

- M. Boquien, J. Borissova, J. Bovy, C. A. Bradna Diaz, W. Nielsen Brandt, J. Brinkmann, J. R. Brownstein, K. Bundy, A. J. Burgasser, E. Burtin, N. G. Busca, C. I. Cañas, M. Cano-Díaz, M. Cappellari, R. Carrera, A. R. Casey, B. C. Sodi, Y. Chen, B. Cherinka, C. Chiappini, P. D. Choi, D. Chojnowski, C. H. Chuang, H. Chung, N. Clerc, R. E. Cohen, J. M. Comerford, J. Comparat, J. C. do Nascimento, L. da Costa, M. C. Cousinou, K. Covey, J. D. Crane, I. Cruz-Gonzalez, K. Cunha, G. S. Ilha, G. J. Damke, J. Darling, J. W. Davidson Jr., K. Dawson, M. A. C. de Icaza Lizaola, A. Macorra, S. de la Torre, N. De Lee, V. Sainte Agathe, A. Deconto Machado, F. Dell'Agli, T. Delubac, A. M. Diamond-Stanic, J. Donor, J. J. Downes, N. Drory, H. Mas des Bourboux, C. J. Duckworth, T. Dwelly, J. Dyer, G. Ebelke, A. D. Eigenbrot, D. J. Eisenstein, Y. P. Elsworth, E. Emsellem, M. Eracleous, G. Erfanianfar, S. Escoffier, X. Fan, E. F. Alvar, J. G. Fernandez-Trincado, R. F. Cirolini, D. Feuillet, A. Finoguenov, S. W. Fleming, A. Font-Ribera, G. Freischlad, P. Frinchaboy, H. Fu, Y. G. M. Chew, L. Galbany, A. E. García Pérez, R. Garcia-Dias, D. A. García-Hernández, L. A. Garma Oehmichen, P. Gaulme, J. Gelfand, H. Gil-Marín, B. A. Gillespie, D. Goddard, J. I. González Hernández, V. Gonzalez-Perez, K. Grabowski, P. J. Green, C. J. Grier, A. Gueguen, H. Guo, J. Guy, A. Hagen, P. Hall, P. Harding, S. Haselquist, S. Hawley, C. R. Hayes, F. Hearty, S. Hekker, J. Hernandez, H. Hernandez Toledo, D. W. Hogg, K. Holley-Bockelmann, J. A. Holtzman, J. Hou, B. C. Hsieh, J. A. S. Hunt, T. A. Hutchinson, H. S. Hwang, C. E. Jimenez Angel, J. A. Johnson, A. Jones, H. Jönsson, E. Jullo, F. Sakil Khan, K. Kinemuchi, D. Kirkby, C. C. Kirkpatrick IV, F. S. Kitaura, G. R. Knapp, J. P. Kneib, J. A. Kollmeier, I. Lacerna, R. R. Lane, D. Lang, D. R. Law, J. M. Le Goff, Y. B. Lee, H. Li, C. Li, J. Lian, Y. Liang, M. Lima, L. Lin, D. Long, S. Lucatello, B. Lundgren, J. T. Mackereth, C. L. MacLeod, S. Mahadevan, M. A. Geimba Maia, S. Majewski, A. Manchado, C. Maraston, V. Mariappan, R. Marques-Chaves, T. Masseron, K. L. Masters, R. M. McDermid, I. D. McGreer, M. Melendez, S. Meneses-Goytia, A. Merloni, M. R. Merrifield, S. Meszaros, A. Meza, I. Minchev, D. Minniti, E. M. Mueller, F. Muller-Sanchez, D. Muna, R. R. Muñoz, A. D. Myers, P. Nair, K. Nandra, M. Ness, J. A. Newman, R. C. Nichol, D. L. Nidever, C. Nitschelm, P. Noterdaeme, J. O'Connell, R. J. Oelkers, A. Oravetz, D. Oravetz, E. A. Ortíz, Y. Osorio, Z. Pace, N. Padilla, N. Palanque-Delabrouille, P. A. Palicio, H. A. Pan, K. Pan, T. Parikh, I. Paris, C. Park, S. Peirani, M. Pellejero-Ibanez, S. Penny, W. J. Percival, I. Perez-Fournon, P. Petitjean, M. M. Pieri, M. Pinsonneault, A. Pisani, F. Prada, A. Prakash, A. B. de Andrade Queiroz, M. J. Raddick, A. Raichoor, S. B. Rembold, H. Richstein, R. A. Riffel, R. Riffel, H. W. Rix, A. C. Robin, S. R. Torres, C. Román-Zúñiga, A. J. Ross, G. Rossi, J. Ruan, R. Ruggeri, J. Ruiz, M. Salvato, A. G. Sánchez, S. F. Sánchez, J. S. Almeida, J. R. Sánchez-Gallego, F. A. S. Rojas, B. X. Santiago, R. P. Schiavon, J. S. Schimoia, E. Schlafly, D. Schlegel, D. P. Schneider, W. J. Schuster, A. Schwope, H. J. Seo, A. Serenelli, S. Shen, Y. Shen, M. Shetrone, M. Shull, V. S. Aguirre, J. D. Simon, M. Skrutskie, A. Slosar, R. Smethurst, V. Smith, J. Sobeck, G. Somers, B. J. Souter, D. Souto, A. Spindler, D. V. Stark, K. Stassun, M. Steinmetz, D. Stello, T. Storchi-Bergmann, A. Streblyanska, G. S. Stringfellow, G. Suárez, J. Sun, L. Szigeti, M. Taghizadeh-Popp, M. S. Talbot, B. Tang, C. Tao, J. Tayar, M. Tembe, J. Teske, A. R. Thakar, D. Thomas, P. Tissera, R. Tojeiro, C. Tremonti, N. W. Troup, M. Urry, O. Valenzuela, R. Bosch, J. Vargas-González, M. Vargas-Magaña, J. A. Vazquez, S. Villanova, N. Vogt, D. Wake, Y. Wang, B. A. Weaver, A. M. Weijmans, D. H. Weinberg, K. B. Westfall, D. G. Whelan, E. Wilcots, V. Wild, R. A. Williams, J. Wilson, W. M. Wood-Vasey, D. Wylezalek, T. Xiao, R. Yan, M. Yang, J. E. Ybarra, C. Yéche, N. Zakkamska, O. Zamora, P. Zarrouk, G. Zasowski, K. Zhang, C. Zhao, G. B. Zhao, Z. Zheng, Z. Zheng, Z. M. Zhou, G. Zhu, J. C. Zinn, and H. Zou, *Astrophys. J. Suppl. Ser.* **235**, 42 (2018), arXiv: [1707.09322](#).
- 148 D. J. Schlegel, D. P. Finkbeiner, and M. Davis, *Astrophys. J.* **500**, 525 (1998), arXiv: [astro-ph/9710327](#).
- 149 T. M. C. Abbott, M. Adamów, M. Aguena, S. Allam, A. Amon, J. Annis, S. Avila, D. Bacon, M. Banerji, K. Bechtol, M. R. Becker, G. M. Bernstein, E. Bertin, S. Bhargava, S. L. Bridle, D. Brooks, D. L. Burke, A. Carnero Rosell, M. Carrasco Kind, J. Carretero, F. J. Castander, R. Cawthon, C. Chang, A. Choi, C. Conselice, M. Costanzi, M. Crocce, L. N. da Costa, T. M. Davis, J. De Vicente, J. DeRose, S. Desai, H. T. Diehl, J. P. Dietrich, A. Drlica-Wagner, K. Eckert, J. Elvin-Poole, S. Everett, A. E. Evrard, I. Ferrero, A. Ferté, B. Flaugher, P. Fosalba, D. Friedel, J. Frieman, J. García-Bellido, E. Gaztanaga, L. Gelman, D. W. Gerdes, T. Giannantonio, M. S. S. Gill, D. Gruen, R. A. Gruendl, J. Gschwend, G. Gutierrez, W. G. Hartley, S. R. Hinton, D. L. Hollowood, K. Honscheid, D. Huterer, D. J. James, T. Jeltema, M. D. Johnson, S. Kent, R. Kron, K. Kuehn, N. Kuropatkin, O. Lahav, T. S. Li, C. Lidman, H. Lin, N. MacCrann, M. A. G. Maia, T. A. Manning, J. D. Maloney, M. March, J. L. Marshall, P. Martini, P. Melchior, F. Menanteau, R. Miquel, R. Morgan, J. Myles, E. Neilsen, R. L. C. Ogando, A. Palmese, F. Paz-Chinchón, D. Petracick, A. Pieres, A. A. Plazas, C. Pond, M. Rodriguez-Monroy, A. K. Romer, A. Roodman, E. S. Rykoff, M. Sako, E. Sanchez, B. Santiago, V. Scarpine, S. Serrano, I. Sevilla-Noarbe, J. A. Smith, M. Smith, M. Soares-Santos, E. Suchyta, M. E. C. Swanson, G. Tarle, D. Thomas, C. To, P. E. Tremblay, M. A. Troxel, D. L. Tucker, D. J. Turner, T. N. Varga, A. R. Walker, R. H. Wechsler, J. Weller, W. Wester, R. D. Wilkinson, B. Yanny, Y. Zhang, R. Nikutta, M. Fitzpatrick, A. Jacques, A. Scott, K. Olsen, L. Huang, D. Herrera, S. Juneau, D. Nidever, B. A. Weaver, C. Adean, V. Correia, M. de Freitas, F. N. Freitas, C. Singulani, and G. Vila-Verde, *Astrophys. J. Suppl. Ser.* **255**, 20 (2021), arXiv: [2101.05765](#).
- 150 151 T. M. C. Abbott, F. B. Abdalla, S. Allam, A. Amara, J. Annis, J. Asorey, S. Avila, O. Ballester, M. Banerji, W. Barkhouse, L. Baruah, M. Baumer, K. Bechtol, M. R. Becker, A. Benoit-Lévy, G. M. Bernstein, E. Bertin, J. Blazek, S. Bocquet, D. Brooks, D. Brout, E. Buckley-Geer, D. L. Burke, V. Busti, R. Campisano, L. Cardiel-Sas, A. C. Rosell, M. C. Kind, J. Carretero, F. J. Castander, R. Cawthon, C. Chang, X. Chen, C. Conselice, G. Costa, M. Crocce, C. E. Cunha, C. B. DAndrea, L. N. Costa, R. Das, G. Daues, T. M. Davis, C. Davis, J. D. Vicente, D. L. DePoy, J. DeRose, S. Desai, H. T. Diehl, J. P. Dietrich, S. Dodelson, P. Doel, A. Drlica-Wagner, T. F. Eifler, A. E. Elliott, A. E. Evrard, A. Farahi, A. F. Neto, E. Fernandez, D. A. Finley, B. Flaugher, R. J. Foley, P. Fosalba, D. N. Friedel, J. Frieman, J. García-Bellido, E. Gaztanaga, D. W. Gerdes, T. Giannantonio, M. S. S. Gill, K. Glazebrook, D. A. Goldstein, M. Gower, D. Gruen, R. A. Gruendl, J. Gschwend, R. R. Gupta, G. Gutierrez, S. Hamilton, W. G. Hartley, S. R. Hinton, J. M. Hislop, D. Hollowood, K. Honscheid, B. Hoyle, D. Huterer, B. Jain, D. J. James, T. Jeltema, M. W. G. Johnson, M. D. Johnson, T. Kacprzak, S. Kent, G. Khullar, M. Klein, A. Kovacs, A. M. G. Koziol, E. Krause, A. Kremin, R. Kron, K. Kuehn, S. Kuhlmann, N. Kuropatkin, O. Lahav, J. Lasker, T. S. Li, R. T. Li, A. R. Liddle, M. Lima, H. Lin, P. López-Reyes, N. MacCrann, M. A. G. Maia, J. D. Maloney, M. Manera, M. March,

- J. Marriner, J. L. Marshall, P. Martini, T. McClintock, T. McKay, R. G. McMahon, P. Melchior, F. Menanteau, C. J. Miller, R. Miquel, J. J. Mohr, E. Morganson, J. Mould, E. Neilsen, R. C. Nichol, F. Nogueira, B. Nord, P. Nugent, L. Nunes, R. L. C. Ogando, L. Old, A. B. Pace, A. Palmese, F. Paz-Chinchón, H. V. Peiris, W. J. Percival, D. Petrvack, A. A. Plazas, J. Poh, C. Pond, A. Porredon, A. Pujol, A. Refregier, K. Reil, P. M. Ricker, R. P. Rollins, A. K. Romer, A. Roodman, P. Rooney, A. J. Ross, E. S. Rykoff, M. Sako, M. L. Sanchez, E. Sanchez, B. Santiago, A. Saro, V. Scarpine, D. Scolnic, S. Serrano, I. Sevilla-Noarbe, E. Sheldon, N. Shipp, M. L. Silveira, M. Smith, R. C. Smith, J. A. Smith, M. Soares-Santos, F. Sobreira, J. Song, A. Stebbins, E. Suchyta, M. Sullivan, M. E. C. Swanson, G. Tarle, J. Thaler, D. Thomas, R. C. Thomas, M. A. Troxel, D. L. Tucker, V. Vikram, A. K. Vivas, A. R. Walker, R. H. Wechsler, J. Weller, W. Wester, R. C. Wolf, H. Wu, B. Yanny, A. Zenteno, Y. Zhang, J. Zuntz, S. Juneau, M. Fitzpatrick, R. Nikutta, D. Nidever, K. Olsen, and A. Scott, *Astrophys. J. Suppl. Ser.* **239**, 18 (2018), arXiv: [1801.03181](#).
- 152 S. Arnouts, S. Cristiani, L. Moscardini, S. Matarrese, F. Lucchin, A. Fontana, and E. Giallongo, *Mon. Not. R. Astron. Soc.* **310**, 540 (1999), arXiv: [astro-ph/9902290](#).
- 153 O. Ilbert, S. Arnouts, H. J. McCracken, M. Bolzonella, E. Bertin, O. Le Fèvre, Y. Mellier, G. Zamorani, R. Pelló, A. Iovino, L. Tresse, V. Le Brun, D. Bottini, B. Garilli, D. Maccagni, J. P. Picat, R. Scaramella, M. Scoggio, G. Vettolani, A. Zanichelli, C. Adami, S. Bardelli, A. Cappi, S. Charlot, P. Ciliegi, T. Contini, O. Cucciati, S. Foucaud, P. Franzetti, I. Gavignaud, L. Guzzo, B. Marano, C. Marinoni, A. Mazure, B. Meneux, R. Merighi, S. Paltani, A. Pollo, L. Pozzetti, M. Radovich, E. Zucca, M. Bondi, A. Bongiorno, G. Busarello, S. De La Torre, L. Gregorini, F. Lamareille, G. Mathez, P. Merluzzi, V. Riipépi, D. Rizzo, and D. Vergani, *Astron. Astrophys.* **457**, 841 (2006).
- 154 G. Bruzual, and S. Charlot, *Mon. Not. R. Astron. Soc.* **344**, 1000 (2003), arXiv: [astro-ph/0309134](#).
- 155 G. Chabrier, *Publ. Astron. Soc. Pac.* **115**, 763 (2003), arXiv: [astro-ph/0304382](#).
- 156 D. Calzetti, A. L. Kinney, and T. Storchi-Bergmann, *Astrophys. J.* **429**, 582 (1994).
- 157 C. Maraston, J. Pforr, B. M. Henriques, D. Thomas, D. Wake, J. R. Brownstein, D. Capozzi, J. Tinker, K. Bundy, R. A. Skibba, A. Beifiori, R. C. Nichol, E. Edmondson, D. P. Schneider, Y. Chen, K. L. Masters, O. Steele, A. S. Bolton, D. G. York, B. A. Weaver, T. Higgs, D. Bizyaev, H. Brewington, E. Malanushenko, V. Malanushenko, S. Snedden, D. Oravetz, K. Pan, A. Shelden, and A. Simmons, *Mon. Not. R. Astron. Soc.* **435**, 2764 (2013), arXiv: [1207.6114](#).
- 158 C. Maraston, *Mon. Not. R. Astron. Soc.* **362**, 799 (2005), arXiv: [astro-ph/0410207](#).
- 159 C. Maraston, G. Strömbäck, D. Thomas, D. A. Wake, and R. C. Nichol, *Mon. Not. R. Astron. Soc.-Lett.* **394**, L107 (2009), arXiv: [0809.1867](#).
- 160 R. Abbott, et al. (LIGO Scientific Collaboration and Virgo Collaboration), *Astrophys. J. Lett.* **913**, L7 (2021), arXiv: [2010.14533](#).
- 161 C. Talbot, and E. Thrane, *Astrophys. J.* **856**, 173 (2018), arXiv: [1801.02699](#).
- 162 B. P. Abbott, et al. (LIGO Scientific Collaboration and Virgo Collaboration), *Astrophys. J.* **882**, L24 (2019), arXiv: [1811.12940](#).
- 163 J. Roulet, and M. Zaldarriaga, *Mon. Not. R. Astron. Soc.* **484**, 4216 (2019), arXiv: [1806.10610](#).
- 164 M. Fishbach, and D. E. Holz, *Astrophys. J.* **891**, L27 (2020), arXiv: [1905.12669](#).
- 165 A. Mangiagli, A. Klein, A. Sesana, E. Barausse, and M. Colpi, *Phys. Rev. D* **99**, 064056 (2019), arXiv: [1811.01805](#).
- 166 A. Nishizawa, E. Berti, A. Klein, and A. Sesana, *Phys. Rev. D* **94**, 064020 (2016), arXiv: [1605.01341](#).
- 167 M. Hannam, P. Schmidt, A. Bohé, L. Haegel, S. Husa, F. Ohme, G. Pratten, and M. Pürrer, *Phys. Rev. Lett.* **113**, 151101 (2014), arXiv: [1308.3271](#).
- 168 Z.-C. Liang, Y.-M. Hu, Y. Jiang, J. Cheng, J.-D. Zhang, and J. Mei, arXiv: [2107.08643](#).
- 169 J. He, *Phys. Rev. D* **100**, 023527 (2019), arXiv: [1903.11254](#).
- 170 C. Howlett, and T. M. Davis, *Mon. Not. R. Astron. Soc.* **492**, 3803 (2020), arXiv: [1909.00587](#).
- 171 C. Nicolaou, O. Lahav, P. Lemos, W. Hartley, and J. Braden, *Mon. Not. R. Astron. Soc.* **495**, 90 (2020), arXiv: [1909.09609](#).
- 172 S. Mukherjee, G. Lavaux, F. R. Bouchet, J. Jasche, B. D. Wandelt, S. Nissanke, F. Leclercq, and K. Hotokezaka, *Astron. Astrophys.* **646**, A65 (2021), arXiv: [1909.08627](#).
- 173 Y. Gong, X. Liu, Y. Cao, X. Chen, Z. Fan, R. Li, X. D. Li, Z. Li, X. Zhang, and H. Zhan, *Astrophys. J.* **883**, 203 (2019), arXiv: [1901.04634](#).
- 174 D. Foreman-Mackey, D. W. Hogg, D. Lang, and J. Goodman, *Publ. Astron. Soc. Pac.* **125**, 306 (2013), arXiv: [1202.3665](#).
- 175 D. Foreman-Mackey, W. Farr, M. Sinha, A. Archibald, D. Hogg, J. Sanders, J. Zuntz, P. Williams, A. Nelson, M. de Val-Borro, T. Erhardt, I. Pashchenko, and O. Pla, *J. Open Source Softw.* **4**, 1864 (2019), arXiv: [1911.07688](#).
- 176 D. Q. Su, X. Cui, Y. Wang, and Z. Yao, Advanced Technology Optical/IR Telescopes VI, in *Society of Photo-Optical Instrumentation Engineers (SPIE) Conference Series*, edited by L. M. Stepp (1998), pp. 76–90.
- 177 X. Q. Cui, Y. H. Zhao, Y. Q. Chu, G. P. Li, Q. Li, L. P. Zhang, H. J. Su, Z. Q. Yao, Y. N. Wang, X. Z. Xing, X. N. Li, Y. T. Zhu, G. Wang, B. Z. Gu, A. L. Luo, X. Q. Xu, Z. C. Zhang, G. R. Liu, H. T. Zhang, D. H. Yang, S. Y. Cao, H. Y. Chen, J. J. Chen, K. X. Chen, Y. Chen, J. R. Chu, L. Feng, X. F. Gong, Y. H. Hou, H. Z. Hu, N. S. Hu, Z. W. Hu, L. Jia, F. H. Jiang, X. Jiang, Z. B. Jiang, G. Jin, A. H. Li, Y. Li, Y. P. Li, G. Q. Liu, Z. G. Liu, W. Z. Lu, Y. D. Mao, L. Men, Y. J. Qi, Z. X. Qi, H. M. Shi, Z. H. Tang, Q. S. Tao, D. Q. Wang, D. Wang, G. M. Wang, H. Wang, J. N. Wang, J. Wang, J. L. Wang, J. P. Wang, L. Wang, S. Q. Wang, Y. Wang, Y. F. Wang, L. Z. Xu, Y. Xu, S. H. Yang, Y. Yu, H. Yuan, X. Y. Yuan, C. Zhai, J. Zhang, Y. X. Zhang, Y. Zhang, M. Zhao, F. Zhou, G. H. Zhou, J. Zhu, and S. C. Zou, *Res. Astron. Astrophys.* **12**, 1197 (2012).
- 178 G. Zhao, Y. H. Zhao, Y. Q. Chu, Y. P. Jing, and L. C. Deng, *Res. Astron. Astrophys.* **12**, 723 (2012).
- 179 A. Aghamousa, et al. (DESI Collaboration), arXiv: [1611.00036](#).
- 180 R. S. de Jong, O. Bellido-Tirado, C. Chiappini, É. Depagne, R. Haynes, D. Johl, O. Schnurr, A. Schwone, J. Walcher, F. Dionies, D. Haynes, A. Kelz, F. S. Kitaura, G. Lamer, I. Minchev, V. Müller, S. E. Nuza, J.-C. Olaya, T. Piffl, E. Popow, M. Steinmetz, U. Ural, M. Williams, R. Winkler, L. Wisotzki, W. R. Ansorg, M. Banerji, E. G. Solares, M. Irwin, R. C. Kennicutt Jr, D. King, R. McMahon, S. Koposov, I. R. Parry, N. A. Walton, G. Finger, O. Iwert, M. Krumpe, J.-L. Lizón, M. Vincenzo, J.-P. Amans, P. Bonifacio, M. Cohen, P. Francois, P. Jagourel, S. B. Mignot, F. Royer, P. Sartoretti, R. Bender, F. Grupp, H.-J. Hess, F. L. Bardl, B. Muschielok, H. Böhringer, T. Boller, A. Bongiorno, M. Brusa, T. Dwelly, A. Merloni, K. Nandra, M. Salvato, J. H. Pragt, R. Navarro, G. Gerlofsma, R. Roelfsema, G. B. Dalton, K. F. Middleton, I. A. Tosh, C. Boeche, E. Caffau, N. Christlieb, E. K. Grebel, C. Hansen, A. Koch, H.-G. Ludwig, A. Quirrenbach, L. Sbordone, W. Seifert, G. Thimm, T. Trifonov, A. Helmi, S. C. Trager, S. Feltzing, A. Korn, and W. Boland, Proc. SPIE Int. Soc. Opt. Eng. **8446**, 84460T (2012).
- 181 E. da Cunha, A. M. Hopkins, M. Colless, E. N. Taylor, C. Blake, C. Howlett, C. Magoulas, J. R. Lucey, C. Lagos, K. Kuehn, Y. Gordon, D. Barat, F. Bian, C. Wolf, M. J. Cowley, M. White, I. Achitou, M. Bilicki, J. Bland-Hawthorn, K. Bolejko, M. J. I. Brown, R. Brown, J. Bryant, S. Croom, T. M. Davis, S. P. Driver, M. D. Filipovic, S. R. Hinton, M. Johnston-Hollitt, D. H. Jones, B. Koribalski, D. Kleiner, J. Lawrence, N. Lorente, J. Mould, M. S. Owers, K. Pimbblet, C. G. Tinney, N. F. H. Tohill, and F. Watson, *Publ. Astron. Soc. Aust.* **34**, e047 (2017), arXiv: [1706.01246](#).
- 182 J. P. Gardner, J. C. Mather, M. Clampin, R. Doyon, M. A. Greenhouse, H. B. Hammel, J. B. Hutchings, P. Jakobsen, S. J. Lilly, K. S. Long, J. I. Lunine, M. J. McCaughey, M. Mountain, J. Nella,

- G. H. Rieke, M. J. Rieke, H. W. Rix, E. P. Smith, G. Sonneborn, M. Stiavelli, H. S. Stockman, R. A. Windhorst, and G. S. Wright, *Space Sci. Rev.* **123**, 485 (2006), arXiv: [astro-ph/0606175](#).
- 183 J. Kalirai, *Contemp. Phys.* **59**, 251 (2018), arXiv: [1805.06941](#).
- 184 J. Green, P. Schechter, C. Baltay, R. Bean, D. Bennett, R. Brown, C. Conselice, M. Donahue, X. Fan, B. S. Gaudi, C. Hirata, J. Kalirai, T. Lauer, B. Nichol, N. Padmanabhan, S. Perlmutter, B. Rauscher, J. Rhodes, T. Roellig, D. Stern, T. Sumi, A. Tanner, Y. Wang, D. Weinberg, E. Wright, N. Gehrels, R. Sambruna, W. Traub, J. Anderson, K. Cook, P. Garnavich, L. Hillenbrand, Z. Ivezić, E. Kerins, J. Lunine, P. McDonald, M. Penny, M. Phillips, G. Rieke, A. Riess, R. van der Marel, R. K. Barry, E. Cheng, D. Content, R. Cutri, R. Goullioud, K. Grady, G. Helou, C. Jackson, J. Kruk, M. Melton, C. Peddie, N. Rioux, and M. Seiffert, arXiv: [1208.4012](#).
- 185 R. Chary, G. Helou, G. Brammer, P. Capak, A. Faisst, D. Flynn, S. Groom, H. C. Ferguson, C. Grillmair, S. Hemmati, A. Koekemoer, B. Lee, S. Malhotra, H. Miyatake, P. Melchior, I. Momcheva, J. Newman, J. Masiero, R. Paladini, A. Prakash, B. Rusholme, N. R. Stickley, A. Smith, W. M. Wood-Vasey, and H. I. Teplitz, arXiv: [2008.10663](#).
- 186 D. S. Sivia, and J. Skilling, *Information Gain: Quantifying the Worth of an Experiment*, chapter 7, 163–164, 2nd edition (Oxford University Press, Oxford, 2006).
- 187 W. F. Feng, H. T. Wang, X. C. Hu, Y. M. Hu, and Y. Wang, *Phys. Rev. D* **99**, 123002 (2019), arXiv: [1901.02159](#).
- 188 W. H. Ruan, C. Liu, Z. K. Guo, Y. L. Wu, and R. G. Cai, *Nat. Astron.* **4**, 108 (2020), arXiv: [2002.03603](#).
- 189 W. H. Ruan, C. Liu, Z. K. Guo, Y. L. Wu, and R. G. Cai, *Research* **2021**, 1 (2021).
- 190 R. M. O’Leary, F. A. Rasio, J. M. Fregeau, N. Ivanova, and R. O’Shaughnessy, *Astrophys. J.* **637**, 937 (2006), arXiv: [astro-ph/0508224](#).
- 191 K. Kremer, S. Chatterjee, K. Breivik, C. L. Rodriguez, S. L. Larson, and F. A. Rasio, *Phys. Rev. Lett.* **120**, 191103 (2018), arXiv: [1802.05661](#).
- 192 L. Barack, and C. Cutler, *Phys. Rev. D* **69**, 082005 (2004), arXiv: [gr-qc/0310125](#).
- 193 X. Chen, and P. Amaro-Seoane, *Astrophys. J.* **842**, L2 (2017), arXiv: [1702.08479](#).
- 194 L. Randall, and Z. Z. Xianyu, *Astrophys. J.* **914**, 75 (2021), arXiv: [1907.02283](#).
- 195 V. Gayathri, J. Healy, J. Lange, B. O’Brien, M. Szczepanczyk, I. Bartos, M. Campanelli, S. Klimenko, C. Lousto, and R. O’Shaughnessy, arXiv: [2009.05461](#).
- 196 V. Gayathri, J. Healy, J. Lange, B. O’Brien, M. Szczepanczyk, I. Bartos, M. Campanelli, S. Klimenko, C. Lousto, and R. O’Shaughnessy, arXiv: [2009.14247](#).
- 197 J. Samsing, and D. J. D’Orazio, *Mon. Not. R. Astron. Soc.* **481**, 5445 (2018), arXiv: [1804.06519](#).
- 198 K. N. Abazajian, J. K. Adelman-McCarthy, M. A. Agüeros, S. S. Allam, C. A. Prieto, D. An, K. S. J. Anderson, S. F. Anderson, J. Annis, N. A. Bahcall, C. A. L. Bailer-Jones, J. C. Barentine, B. A. Bassett, A. C. Becker, T. C. Beers, E. F. Bell, V. Belokurov, A. A. Berlind, E. F. Berman, M. Bernardi, S. J. Bickerton, D. Bizyaev, J. P. Blakeslee, M. R. Blanton, J. J. Bochanski, W. N. Boroski, H. J. Brewington, J. Brinchmann, J. Brinkmann, R. J. Brunner, T. Budavári, L. N. Carey, S. Carliles, M. A. Carr, F. J. Castander, D. Cinabro, A. J. Connolly, I. Csabai, C. E. Cunha, P. C. Czarapata, J. R. A. Davenport, E. de Haas, B. Dilday, M. Doi, D. J. Eisenstein, M. L. Evans, N. W. Evans, X. Fan, S. D. Friedman, J. A. Frieman, M. Fukugita, B. T. Gänsicke, E. Gates, B. Gillespie, G. Gilmore, B. Gonzalez, C. F. Gonzalez, E. K. Grebel, J. E. Gunn, Z. Györy, P. B. Hall, P. Harding, F. H. Harris, M. Harvanek, S. L. Hawley, J. J. E. Hayes, T. M. Heckman, J. S. Hendry, G. S. Hennessy, R. B. Hindsley, J. Hoblitt, C. J. Hogan, D. W. Hogg, J. A. Holtzman, J. B. Hyde, S. Ichikawa, T. Ichikawa, M. Im, Ž. Ivezić, S. Jester, L. Jiang, J. A. Johnson, A. M. Jorgensen, M. Jurić, S. M. Kent, R. Kessler, S. J. Kleinman, G. R. Knapp, K. Konishi, R. G. Kron, J. Krzesinski, N. Kuropatkin, H. Lampeitl, S. Lebedeva, M. G. Lee, Y. S. Lee, R. F. Leger, S. Lépine, N. Li, M. Lima, H. Lin, D. C. Long, C. P. Loomis, J. Loveday, R. H. Lupton, E. Magnier, O. Malanushenko, V. Malanushenko, R. Mandelbaum, B. Margon, J. P. Marriner, D. Martínez-Delgado, T. Matsubara, P. M. McGehee, T. A. McKay, A. Meiksin, H. L. Morrison, F. Mullally, J. A. Munn, T. Murphy, T. Nash, A. Nebo, E. H. Neilsen, H. J. Newberg, P. R. Newman, R. C. Nichol, T. Nicinski, M. Nieto-Santisteban, A. Nitta, S. Okamura, D. J. Oravetz, J. P. Ostriker, R. Owen, N. Padmanabhan, K. Pan, C. Park, G. Pauls, J. Peoples, W. J. Percival, J. R. Pier, A. C. Pope, D. Pourbaix, P. A. Price, N. Purger, T. Quinn, M. J. Raddick, P. R. Fiorentin, G. T. Richards, M. W. Richmond, A. G. Riess, H. W. Rix, C. M. Rockosi, M. Sako, D. J. Schlegel, D. P. Schneider, R. D. Scholz, M. R. Schreiber, A. D. Schwope, U. Seljak, B. Sesar, E. Sheldon, K. Shimasaku, V. C. Sibley, A. E. Simmons, T. Sivarani, J. A. Smith, M. C. Smith, V. Smolčić, S. A. Snedden, A. Stebbins, M. Steinmetz, C. Stoughton, M. A. Strauss, M. SubbaRao, Y. Suto, A. S. Szalay, I. Szapudi, P. Szkody, M. Tanaka, M. Tegmark, L. F. A. Teodoro, A. R. Thakar, C. A. Tremonti, D. L. Tucker, A. Uomoto, D. E. Vanden Berk, J. Vandenberg, S. Vidrih, M. S. Vogeley, W. Voges, N. P. Vogt, Y. Wadadekar, S. Watters, D. H. Weinberg, A. A. West, S. D. M. White, B. C. Wilhite, A. C. Wonders, B. Yanny, D. R. Yocom, D. G. York, I. Zehavi, S. Zibetti, and D. B. Zucker, *Astrophys. J. Suppl. Ser.* **182**, 543 (2009), arXiv: [0812.0649](#).
- 199 J. De Vicente, E. Sánchez, and I. Sevilla-Noarbe, *Mon. Not. R. Astron. Soc.* **459**, 3078 (2016), arXiv: [1511.07623](#).
- 200 V. De Luca, G. Franciolini, P. Pani, and A. Riotto, *J. Cosmol. Astropart. Phys.* **2020**, 44 (2020), arXiv: [2005.05641](#).
- 201 S. Clesse, and J. Garcia-Bellido, arXiv: [2007.06481](#).
- 202 V. De Luca, V. Desjacques, G. Franciolini, P. Pani, and A. Riotto, *Phys. Rev. Lett.* **126**, 051101 (2021), arXiv: [2009.01728](#).
- 203 V. De Luca, G. Franciolini, P. Pani, and A. Riotto, *J. Cosmol. Astropart. Phys.* **2021**, 3 (2021), arXiv: [2102.03809](#).
- 204 H. Deng, *J. Cosmol. Astropart. Phys.* **2021**, 58 (2021), arXiv: [2101.11098](#).
- 205 M. Visser, *Class. Quantum Grav.* **21**, 2603 (2004), arXiv: [gr-qc/0309109](#).
- 206 Y. Gong, *Class. Quantum Grav.* **22**, 2121 (2005), arXiv: [astro-ph/0405446](#).
- 207 E. K. Li, M. Du, Z. H. Zhou, H. Zhang, and L. Xu, *Mon. Not. R. Astron. Soc.* **501**, 4452 (2021), arXiv: [1911.12076](#).
- 208 I. Bartos, A. P. S. Crotts, and S. Márka, *Astrophys. J.* **801**, L1 (2015), arXiv: [1410.0677](#).
- 209 H. Y. Chen, and D. E. Holz, *Astrophys. J.* **840**, 88 (2017), arXiv: [1509.00055](#).
- 210 N. J. Klingler, J. A. Kennea, P. A. Evans, A. Tohuvavohu, S. B. Cenko, S. D. Barthelmy, A. P. Beardmore, A. A. Breeveld, P. J. Brown, D. N. Burrows, S. Campana, G. Cusumano, A. D’ái, P. D’Avanzo, V. D’Elia, M. de Pasquale, S. W. K. Emery, J. Garcia, P. Giommi, C. Gronwall, D. H. Hartmann, H. A. Krimm, N. P. M. Kuin, A. Lien, D. B. Malesani, F. E. Marshall, A. Melandri, J. A. Nousek, S. R. Oates, P. T. O’Brien, J. P. Osborne, K. L. Page, D. M. Palmer, M. Perri, J. L. Racusin, M. H. Siegel, T. Sakamoto, B. Sbarufatti, G. Tagliaferri, and E. Troja, *Astrophys. J. Suppl. Ser.* **245**, 15 (2019), arXiv: [1909.11586](#).
- 211 T. Abbott, et al. (DES), arXiv: [astro-ph/0510346](#).
- 212 I. Sevilla-Noarbe, K. Bechtol, M. Carrasco Kind, A. Carnero Rosell, M. R. Becker, A. Drlica-Wagner, R. A. Gruendl, E. S. Rykoff, E. Sheldon, B. Yanny, A. Alarcon, S. Allam, A. Amon, A. Benoit-Lévy, G. M. Bernstein, E. Bertin, D. L. Burke, J. Carretero, A. Choi, H. T. Diehl, S. Everett, B. Flaugher, E. Gaztanaga, J. Gschwend, I. Harrison, W. G. Hartley, B. Hoyle, M. Jarvis, M. D. Johnson, R. Kessler, R. Kron, N. Kuropatkin, B. Leistedt, T. S. Li, F. Menanteau, E. Morgan, R. L. C. Ogando, A. Palmese, F. Paz-Chinchón, A. Pieres, C. Pond, M. Rodriguez-Monroy, J. A. Smith, K. M. Stringer, M. A. Troxel, D. L. Tucker, J. de Vicente, W. Wester, Y. Zhang, T. M. C.

- Abbott, M. Aguena, J. Annis, S. Avila, S. Bhargava, S. L. Bridle, D. Brooks, D. Brout, F. J. Castander, R. Cawthon, C. Chang, C. Conselice, M. Costanzi, M. Crocce, L. N. da Costa, M. E. S. Pereira, T. M. Davis, S. Desai, J. P. Dietrich, P. Doel, K. Eckert, A. E. Evrard, I. Ferrero, P. Fosalba, J. García-Bellido, D. W. Gerdes, T. Giannantonio, D. Gruen, G. Gutierrez, S. R. Hinton, D. L. Hollowood, K. Honscheid, E. M. Huff, D. Huterer, D. J. James, T. Jeltema, K. Kuehn, O. Lahav, C. Lidman, M. Lima, H. Lin, M. A. G. Maia, J. L. Marshall, P. Martini, P. Melchior, R. Miquel, J. J. Mohr, R. Morgan, E. Neilsen, A. A. Plazas, A. K. Romer, A. Roodman, E. Sanchez, V. Scarpine, M. Schubnell, S. Serrano, M. Smith, E. Suchyta, G. Tarle, D. Thomas, C. To, T. N. Varga, R. H. Wechsler, J. Weller, and R. D. Wilkinson, *Astrophys. J. Suppl. Ser.* **254**, 24 (2021), arXiv: [2011.03407](#).
- 213 C. Zhang, Q. Gao, Y. Gong, D. Liang, A. J. Weinstein, and C. Zhang, *Phys. Rev. D* **100**, 064033 (2019), arXiv: [1906.10901](#).
- 214 A. Toubiana, S. Marsat, S. Babak, J. Baker, and T. Dal Canton, *Phys. Rev. D* **102**, 124037 (2020), arXiv: [2007.08544](#).
- 215 S. Karki, D. Tuyenbayev, S. Kandhasamy, B. P. Abbott, T. D. Abbott, E. H. Anders, J. Berliner, J. Betzwieser, C. Cahillane, L. Canete, C. Conley, H. P. Daveloza, N. De Lillo, J. R. Gleason, E. Goetz, K. Izumi, J. S. Kissel, G. Mendell, V. Quetschke, M. Rodruck, S. Sachdev, T. Sadecki, P. B. Schwinberg, A. Sottile, M. Wade, A. J. Weinstein, M. West, and R. L. Savage, *Rev. Sci. Instrum.* **87**, 114503 (2016), arXiv: [1608.05055](#).
- 216 L. Sun, E. Goetz, J. S. Kissel, J. Betzwieser, S. Karki, A. Viets, M. Wade, D. Bhattacharjee, V. Bossilkov, P. B. Covas, L. E. H. Datrier, R. Gray, S. Kandhasamy, Y. K. Lecoeuche, G. Mendell, T. Mistry, E. Payne, R. L. Savage, A. J. Weinstein, S. Aston, A. Buikema, C. Cahillane, J. C. Driggers, S. E. Dwyer, R. Kumar, and A. Urban, *Class. Quantum Grav.* **37**, 225008 (2020), arXiv: [2005.02531](#).
- 217 D. Estevez, P. Lagabbe, A. Masserot, L. Rolland, M. Seglar-Arroyo, and D. Verkindt, *Class. Quantum Grav.* **38**, 075007 (2021).